# Final report

Project code: B.FLT.0362

Prepared by: Peter Allingham[1], Matthew Dunbabin[1], Eugene McGahan[2], John Valentine[2], Brent Henderson[1], Yang Liu[1], Carly Rosewarne[1]
[1] CSIRO, Australia.
[2] Feedlot Services Australia Pty Ltd.

Date published: October, 2013

ISBN: [Request through Publications Database]

PUBLISHED BY
Meat & Livestock Australia Limited
Locked Bag 991
NORTH SYDNEY NSW 2059

## Characterisation of methane emission from a beef cattle feedlot effluent pond.

Meat & Livestock Australia acknowledges the matching funds provided by the Australian Government to support the research and development detailed in this publication.

## Abstract

Sedimentation ponds, used to collect and store rainfall run-off from cattle feedlot pads, produce a biogas that is mostly methane (74%). However, the contribution to greenhouse gas (GHG) emissions and the cost-benefit of utilising the energy resource are unknown. CSIRO Sensornets Node platform, together with a large floating chamber and low cost sensors provided a capability to report and store simultaneously over the 3G network, real time records of methane emission, key climatic variables and water column temperatures at the pond. Remote logging of methane concentration was facilitated by additional software architecture to monitor and purge the floating chamber. Accumulated 7-day rainfall, resulting in addition of manure feedstock entrained in the run-off, plus water temperatures were the main factors driving methane emission. The estimated ~33.7 tonnes of methane was emitted over the year 2012-13 with the highest emission rate occurring between October and March. The average daily emission rate over this period was 165 g/$m^2$ surface area/d. In contrast, emission rate was 9-fold less (18 g/$m^2$ surface area/d) during the cooler dryer months of April to September. A covered anaerobic pond and boiler system or combined with a heat and power system would have a triple bottom line effect on feedlot profitability if manure feedstock supply was managed and handling costs were $5 -14/tonne manure.

# Executive Summary

This study was commissioned in part, as a consequence of Australian government legislation to target a net reduction in greenhouse gas (GHG) emissions from the rural sector, and in part due to the lack of data to support the development of methodologies for generating offset credits under the Carbon Farming Initiative for the feedlot industry.

Despite research investment into characterising rumen- and manure-based GHG emissions, little was known about the contribution to the total GHG profile of a cattle feedlot as a consequence of the environmentally sound practice of collecting rainfall run-off from feedlot pads and storing it in ponds. These, generally anaerobic ponds, are natural biodigesters that could provide options to minimise GHG emissions by using the methane-rich biogas as an alternative source to fossil fuels for energy generation. Moreover, the cost effectiveness to the producer of such a strategy has not been investigated previously in Australian beef cattle enterprises.

To address the shortfall in knowledge, a feedlot pond was monitored for methane emission over a single annual cycle. This enabled the building of the capacity to monitor, transmit (via the 3G network) and store real-time methane emission data. This was done simultaneously to the transmission and storage of key climatic data and water column temperature data. The site selected was a deep sedimentation pond at a feedlot on the Darling Downs in Queensland. The system, consisted of a floating chamber, low cost sensors, a transmitting weather station and automated control of methane concentration-based capture-purge cycles, and was operated according to audited safety requirements and built-in fail-safe systems.

The study was conducted over a 12-month period (27$^{th}$ April 2012 –26$^{th}$ April 2013) and accumulated 650 individual capture-purge cycles resulting in 161 records of daily average methane emission. Although the pond emitted methane all year round, the rate of emission was influenced significantly by rainfall events and seasonal effects on pond water temperatures. In the warmer, wetter summer months between October and March, mid and lower level water temperature medians in the water column, plus accumulated rainfall, were the primary environmental factors driving emission. In contrast, during the cooler months between April and September, the water surface temperature maxima and minima were the primary factors driving a significantly weaker emission response. During the cooler months the average daily rate of methane emission was 18 g/m$^2$ surface area/d compared to 165 g/m$^2$ surface area/d during the warmer months. The composition of biogas produced from the pond was predominantly methane (74%) with smaller amounts of carbon dioxide (24%) hydrogen sulphide (0.006%) and hydrogen (0.001%).

Phylogenetic profiling of the pond sludge indicated that it contained significant microbial biodiversity. Approximately 85% of the sequences were bacterial in origin, while the remaining 15% were archaeal of which members of the *Methanosaeta* genus were predominant (10.6%). These are acetoclastic methanogens that only make methane from

acetate and are common in anaerobic digesters but are rarely found in the gastrointestinal tract of ruminants.

An economic assessment to determine the feasibility of the feedlot to capture and use the methane as an alternative energy resource was performed by Feedlot Services Australia Pty Ltd (FSA) as a contracted adjunct to the project and their report accompanies this report.

The FSA report provide a synthesis of the methane and climatic data modelled against theoretical and estimated methane yield data to determine the volatile solids (VS) required to provide the yield of methane observed. These data suggested that ~17% of the excreted VS at the feedlot would need to have entered the pond to yield the amount of methane emitted. This was a significantly higher VS than the 2% estimated as a typical amount entrained in feedlot pad runoff. The apparent over-estimation of the methane yield was explained by several caveats: 1) that the prior historical VS in the pond was unknown, 2) that there was a higher methane potential in the runoff leachate than was modelled, 3) that there could be an under prediction of the maximum methane yield and methane conversion factor (MCF) used, and 4) that the average emitting surface area of the sedimentation pond was over estimated. For the purpose of approximating an annual yield of methane from the pond, the emitting surface was arbitrarily set at 1000 $m^2$ although it varied from ~500 $m^2$ to >1500 $m^2$ during the year. Nevertheless, further research is essential in these areas before yields can be accurately assessed and verified.

An economic evaluation was undertaken using scenarios consisting of a covered anaerobic pond (CAP) supplying gas to either a boiler system or a combined heat and power system. Neither scenario was economically feasible for use at the feedlot due to the large variability in methane production, as a result of the variability in feedstock supply to the pond and seasonal effects on air and water temperatures. However, the report also considered a constant feedstock supply scenario where the manure was applied directly to the pond. Under these circumstances, but within defined limits of manure handling costs ($5-14/tonne), both systems were considered economically feasible options. More detail of this assessment is provided in the accompanying FSA report.

Development of strategies, such as metal organic framework technologies to enrich, scrub and store methane/ biogas collected from a CAP-CHP system may further enhance its cost effectiveness. Furthermore, knowledge obtained from studies of microbial dynamics in anaerobic ponds may improve the efficiency of fermentation by selecting and seeding appropriate microbial communities to increase the yield of methane in natural anaerobic digester systems. Further research in these areas is essential.

## Acknowledgements

This work was made possible and achievements against Milestones met due to the unfunded assistance and support of managers, Jim Cudmore, Brad Robinson, Graham Turner and their staff at the Kerwee feedlot.

I acknowledge the contributions made by my CSIRO colleagues, Dr Stephen Sestak for biogas analyses and Ben Mackey, for expert support in the maintenance of the CSIRO Sensornets Node at the Kerwee feedlot.

# Table of Contents

# 1 List of Figures

# 2 List of Tables

# 3 Introduction

Livestock production systems are a leading source of greenhouse gas (GHG) emissions implicated in global warming and climate change. On a global scale, animal industries contribute 37% of methane ($CH_4$), 9% of carbon dioxide ($CO_2$) and 65% of nitrous oxide ($N_2O$) to total gaseous emissions. These combined emissions, when expressed as $CO_2$ equivalents, constitute about 18% of total anthropogenic emissions (FAO, 2009). Fully characterising agricultural emission sources is believed essential to contribute to better informed government policy, and to provide more accuracy to the National GHG inventory. Additionally, better data will facilitate the development of evidence-based methodology in a Carbon Trading future.

Developing and implementing strategies that mitigate agricultural GHG emissions without affecting production gains and cost effectiveness is a realistic pathway to offset the effects of agricultural emissions. Whilst there has been significant research investment into characterising rumen- and manure-based emissions from intensive cattle and dairy production (e.g., Loh *et al*., 2008), little has been invested in defining the contribution to the total GHG emission footprint of feedlots and dairies from the collection and storage of manure-laden rainfall runoff.

Collecting and storing rainfall runoff from the feedlot pad prevents the enriched nutrient (nitrogen (N) and phosphorous (P)) load in the runoff from contaminating ground water. In these circumstances, under anaerobic conditions the volatile solid (VS) in the runoff/slurry is fermented by bacteria and archaea that produce a biogas composed primarily of $CH_4$, but with smaller amounts of $CO_2$ and traces of other gases such as hydrogen sulphide, as by-products of fermentation (Zhongtang *et al*., 2010). These pond systems are thus natural anaerobic digesters and have the potential to be a rich source of methane as renewable energy if covered by an impermeable cover or chamber and then the emissions harvested (Craggs *et al*., 2008; Maranon *et al*., 2011; Minato *et al*., 2012*)*. In addition, use of covers or chambers enable the characterisation of biogas emission as a feasible alternative to monitoring emission plumes using laser spectroscopy.

Beef and dairy manure as a feedstock for $CH_4$ production has a biochemical methane potential (BMP) of 150 - 254 $m^3$ $CH_4$ dry/ $tonne^{-1}$ compared to 279 – 457 $m^3$ $CH_4$/ dry $tonne^{-1}$ for piggery manure (Moller *et al*., 2004; Fujino *et al*., 2005). Methane emissions from dairy slurry storage systems in New Zealand and Japan have been estimated to range from 21.0 – 54.8 g/$m^2$ surface area/d (Craggs *et al*., 2008; Minato *et al*., 2012). However, the manure is generally fresh in these systems and much of the inherent VS would still be present. In contrast, the amount of VS from a feedlot manure pad that actually reaches a storage pond after a rainfall event has been calculated to be 0.5-10% of that excreted onto the pad (McGahan *et al*., 2013; Accompanying FSA report) and thus rates of emission would be expected to be significantly lower. Nonetheless, the potential yield of biogas will depend on the available VS in the pond and vary according to a number of factors including the feedlot diet, the timing of rainfall events in relation to the proportion of fresh and degraded manure entrained in the runoff, and the prior microbial dynamics and VS loading of the pond.

A large capital investment and intensive manure management regimen are required to convert a waste storage system into an anaerobic digester (Neumeier & Mitloehner *et al*., 2013). A comparative life cycle analysis between a beef cattle operation employing an anaerobic digester versus one that did not, indicated a 23% reduction in whole farm GHG emission (Ghafoori *et al*., 2006). Although an economic assessment of burning the biogas for heat and power was not reported, the environmental impact of such a system would be significant.

The principle objectives of the study described herein were to characterise the yield of methane from an anaerobic pond on a Queensland beef feedlot and to assess the seasonal influence on the rate of emission. The study was facilitated by the development of a remote sensing/transmitting capability for collecting real- time data on methane emission into a large floating chamber, on climatic variables from a weather station and water temperature from temperature sensors in the water column.

The data from this study has assisted in an economic assessment and feasibility study of capturing and utilising the biogas by the feedlot. The FSA report should be read in conjunction with the study reported here.

# 4 List of project objectives

1. Construct a floating chamber containing functionally calibrated and validated sensor arrays with telemetry enabling access to a 3G network for continuous or discrete remote data logging cycles.
2. Develop processes for the accurate acquisition of data under field conditions.
3. Develop methods for data handling, transfer and secure long-term storage via the 3G-network server.
4. Confirm the accuracy of sensor measurements using an alternative analytical method (gas chromatography).
5. Data collection cycles
6. Generate a preliminary model for methane output.
7. Report findings and feasibility of “Cap &Capture” to industry (FSA Report).
8. Report the outcomes of the work at industry field days (3) and through industry magazines (Feedback and/or Frontier) and websites (ALFA and MLA sites).

# 5 Methodology

## 5.1 Site Description

Data for methane emission was collected from an anaerobic pond situated at the Kerwee Feedlot, Jondaryan, on the Darling Downs in Queensland. The feedlot has an operating capacity of 8860 SCU[1] and a licensed capacity of 9171 SCU. Runoff from the feedlot pens and feed lanes flow into two sedimentation ponds that overflow into a shallow evaporation pond. The feedlot has the facility to pump water from this area into a retention dam or from the dam back into the ponds or for the irrigation of on-site cultivation. Pond A1 (Figure 1), from which data was collected, receives the runoff from 36 pens and represents 63% of the total feedlot pen catchment area.

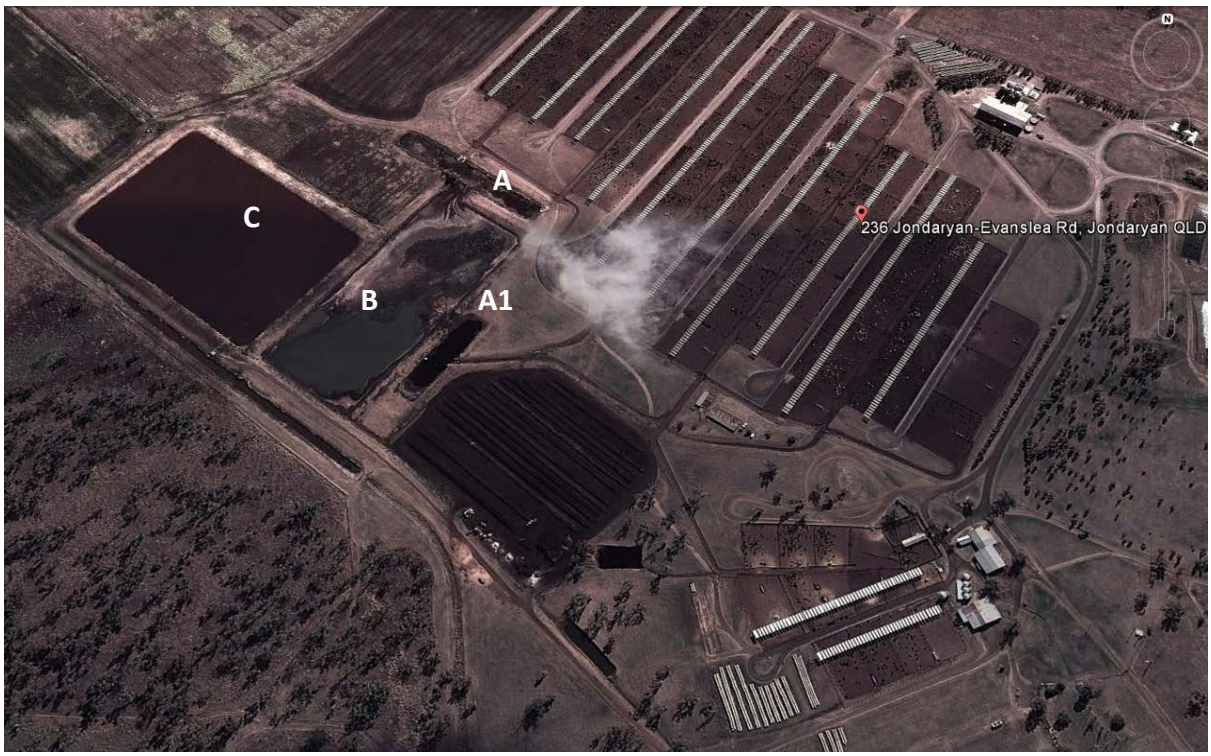


Figure 1 Satellite image (Google Earth) of the Kerwee Feedlot showing runoff sedimentation ponds (A, A1), shallow evaporation pond (B) and storage dam (C).

## 5.2 Pond dimensions and emitting surface

The pond physical dimensions were surveyed by FSA staff in October 2011.

[1] Standard Cattle Unit based on a 600 kg animal.

The dimensions were 110 m x 29 m (crest length by crest width) with the long axis of the pond oriented approximately North-South. The sides of the pond are cambered away from the banks to a narrower bed. Depth at top water level (TWL) is variable and varies with season. At the time of measurement, the average depth of the pond at TWL was 1.8 m with a maximum depth at TWL of 3.9 m. The calculated volume at TWL was reported to be 4.3 ML. Pond dimensions are described in Table 1 of Appendix 1. The pond has never been emptied of sludge in over 12 years of operation. Furthermore, the emitting surface of the pond varied throughout the year with rainfall events, evaporation, and the proportion of dry crusting at the surface, which may or may not inhibit the overall output of the pond or the ebullition of biogas.

The emitting surface of the pond was estimated as the proportion of the total area of the pond that was not crusted during winter and summer. The emitting surface varied from ~500 $m^2$ at the pond's lowest level during winter and ~1600 $m^2$ at its highest level in the summer. For the purpose of estimating a potential annual yield of biogas, the emitting surface area was set at 1000 $m^2$. It is prudent to caution the reader that values of annual methane yield are estimates only.

## 5.3 Estimation of Volatile Solids

. A number of samples of pond sludge were collected at the bottom, at the top and a mid point between on two occasions, October 2011 (n = 51) and September 2012, (n = 12) for the estimation of VS. Dried crust on the banks of the pond was also collected (n = 3) to determine substrate availability if the crust was re-submerged.

. The sludge sampler consisted of a 5 m length of 100 mm PVC piping at the end of which was a chamber enclosed by a spring-loaded sleeve. Opening and releasing the spring-loaded sleeve under water permitted sampling. The entrapped sludge was transferred to plastic containers and held at 4°C until assayed. The VS in the sludge was determined by first oven drying at 103-°C until weight constancy was achieved, followed by ignition at 550°C. The difference in dry weight after ignition was expressed as a percentage of total solids.

## 5.4 Validation of methane emission measurements

To validate remote measured methane emissions, emission was estimated manually by sampling in two-hourly periods, the biogas from five small floating rigs (0.5 m x 0.5 m; Figure 2). The rigs were deployed on transects that subdivided the pond into five regions representing the diversity of the pond environment in terms of depth and amount of sludge. The rigs remained deployed on these transects for the duration of the study. Each rig was equipped with four, sealed PVC cylinders each with a mean headspace of $2.32 \times 10^{-3} \pm 2.13 \times 10^{-5}$ $m^3$ and a sampling surface area of the $7.85 \times 10^{-3}$ $m^2$. At each sampling, 60 mL of atmosphere was extracted through a small port in the top of the cylinder using a gas tight syringe fitted with a 26G needle and transferred into 12 mL evacuated tubes (Exetainer, Labtech, UK). The cylinders were then flushed with fresh air and the rig reset on the pond

before resealing the port with tape. Each rig was sampled three times a day, at ~09.00, ~13.00 and ~16.00, once a month over the 12-month study period.

The percentage methane in the atmosphere of each cylinder was analysed using gas chromatography (Shimadzu) with nitrogen as the carrier gas. The molar volume of methane was adjusted according to Boyle's Ideal Gas Law using the mean ambient temperature during each sampling period. The rate of emission was calculated using the change in mass of the gas over time and expressed as g $CH_4/m^2$ surface/d and compared against the emission rate determined by computation of remote sensing data from the chamber on the same day.


Figure 2 Sampling rigs deployed on the Kerwee pond for sampling of biogas for the manual estimation of rate of methane emission.

There was a strong linear relationship ($R^2$ = 0.954, Figure 3) between manual and remote measurements of methane, confirming that the remote measure of methane emission was both an accurate and a reliable estimate of methane emission from the pond.

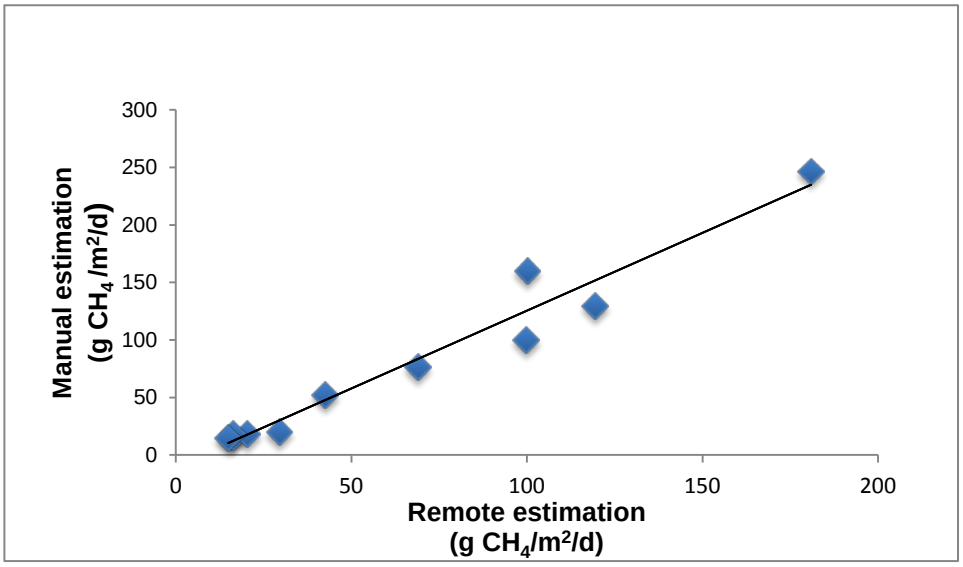


Figure 3 Line of best fit describing the relationship between two methods of estimating methane emission ($r^2$ = 0.954)

## 5.5 Biogas composition

Samples of biogas were collected into 500 mL Tedlar bags or Flexifoil bags using a bubble trap on three separate occasions during the experiment. On two occasions, determination of the composition of the biogas samples was outsourced to SIMTSARS (Queensland Government Department of Natural Resources and Mining, Goodna, Queensland). Additional samples of biogas were collected in Flexifoil bags, plus raw data obtained from SIMTARS, were sent to Dr Stephen Sestak (CSIRO) for additional analyses and computation of air-free values due to unavoidable contamination of samples with air during sampling.

## 5.6 The chamber

The chamber was the top half of a grain silo fitted to a floating pontoon supplied by Clarke Tanks, Dalby. It had an estimated volume of ~4 $m^3$ with an internal diameter of 2.56 m (Figure 4). The chamber was positioned within a ~18 m arc from the pond crest and moved randomly within this defined area each month throughout the year. The length of the ducting used in directing the airflow during purge defined the arc distance.

## 5.7 Node description

The sensor system used in monitoring climatic variables, water column temperatures and methane concentration was setup as a Node located beside the pond. The Node read the environmental sensors including floating chamber methane concentration. The Node was also intrinsic to the control of capturing/purging cycles of the chamber. There was a gateway node located in an office approximately 400 m from the pond, which provided a remote connection to the Internet.

## 5.8 System Layout

The overall system was based on the highly successful automatic methane chambers developed for Seqwater to undertake reservoir ebullitive methane emission quantification. The Seqwater chambers had a total volume of approximately 0.1 $m^3$, with the sensor node and purging system on top of the chamber. The layout of the pond-side system is illustrated in Figure 4.

The most significant challenge of the chamber design and operation was supplying sufficient electrical current from a battery to operate large pneumatic valves, an air compressor and a purging fan. A diesel generator was required to ensure that batteries remained charged during periods of high purge rates.

It was identified that due to the size of the methane chamber and the measurement cycle required, the chamber and immediate area would be considered a hazardous area due to risk of explosion. Therefore, the design of the chamber, selection of sensors and the purging system were required to be intrinsically fail-safe. This was achieved via selection of known intrinsically safe methane sensors (with appropriate explosion proof housing) and pneumatic valves for purging, as well as mechanical and electrical failsafe systems. The overall design was audited and a report supplied by HAZQUIP Australia PTY LTD was filed within the CSIRO HS&E system. To meet the hazardous area safety requirements for safe operation of the floating chamber, both mechanical and electrical fail safe systems were employed. At the chamber, the methane sensor was installed in an approved intrinsically safe housing that allows gas to permeate a membrane to be sensed whilst not posing a flame risk. This only introduces a small time lag to the sensor reading (less than 1 minute), which is much smaller than the time-scales being considered in this analysis.

The core of the chamber failsafe system was a pneumatic solenoid valve, which must be actively closed to allow methane build-up within the chamber. If air and/or electrical power were removed from the solenoid valve the valve was mechanically driven open and the chamber vented through an exhaust to atmosphere. Additionally, to increase the rate at which the chamber was purged, an off-board high-flow rate marine 12 V electric blower (Jabsco Model 35770-Series-Flexmount) was connected to the valve that must be actively turned off to allow the chamber methane concentration to increase. Losing control signal from the sensor node not only opened the valve but also caused the blower to be active. The pneumatic valve and purge system was installed on the floating chamber as illustrated in Figure 5.


Figure 4 Floating chamber and sensor node components.


Figure 5 Fail-safe pneumatic valve and purging system installed on the floating chamber.

## 5.9 Sensors

The sensors used on the floating methane chamber sensor node were chosen to provide methane concentration, pond water column temperature and metrological data. These

sensors were used extensively in a variety of large-scale environmental sensor networks (Dunbabin & Crossman 2010).

The following sections describe the sensors used on the wireless node.

### 5.9.1 Low-cost water temperature sensors

As per the sensor networks used on Lake Wivenhoe and Little Nerang Dam (Dunbabin & Crossman 2010), the floating chamber incorporated a thermistor string through the water column to measure the temperature at various depths.

The low-cost temperature sensor used was a DS28EA00 which is 1-wire digital thermometer developed by Dallas Semiconductor (Maxim Integrated, San Jose, CA) (Figure 5). Communication with this sensor was via a one-wire interface and numerous sensors can be daisy-chained together. Each sensor has a unique 64-bit identification number that is interrogated on startup and its location within the string determined. There were four selectable temperature resolutions available with the sensor ranging from 1/2 to 1/16°C however, the more precise the measurement the longer the individual sample time. The highest precision reading (1/16°C) was selected for these sensors.

The individual temperature sensors were mounted as shown in Figure 6. This small PCB allows soldering of three-core wire between the sensors and has larger holes to provide strain relief using cable ties. These sensors are then encapsulated within a polyurethane resin to ensure they are waterproof. This resin has been found to only introduce ~ 2 minute time constant.


Figure 6 An individual DS28EA00 temperature sensor mounted on a CSIRO PCB (~2-fold magnification).

Figure 6 An individual DS28EA00 temperature sensor mounted on a CSIRO mounting PCB (~2-fold magnification).

Temperature sensors were placed at the surface of the water (T_Water_Surface) and at depths of 0.28 m (Water_T1), 0.74 m (Water_T2), 0.98 m (Water_T3), 1.24 m (Water_T4) and 2.24 m (Water_T5) below the surface in the water column.

### 5.9.2 Vaisala Weather Transmitter (WXT520)

An important feature of the sensor network was that it provided data to facilitate understanding of weather patterns and the affect they have on local processes. A Vaisala weather transmitter WXT520 weather station (Vaisala, Pty. Ltd., Melbourne) was supplied for this project (Figure 7). The WXT520 measures barometric pressure (hPa), relative humidity (%), rainfall (mm), temperature (°C), wind speed (m $s^{-1}$) and direction (for example, 90° is due East while 270° is due West). The transmitter has an extremely low power demand of 3 mA and the sensor uses the SDI-12 communication protocol. Data was collected from the

sensor node every 1-minute and reported back through the sensor network .

Figure 7 The Vaisala WXT520 weather transmitter.

### 5.9.3 Premier Methane Sensor

The floating methane chambers used a certified Premier methane gas sensor from Dynament, UK (Figure 8). These relatively low-cost sensors measure methane concentration in the range 0 to 100% and provide an analog digital converter (ADC) value representing the methane gas concentration in the chamber, and with the electronic circuitry of the gas daughter board shown in Figure 8 the measurement resolution was approximately 0.01 % or 10 ppm.

Figure 8 The Dynament certified methane sensor.

In the Dunbabin & Crossman (2010) study, the methane sensor was powered down to save power whilst not measuring. However, it was found that the sensors lost measurement accuracy and calibration in environments of high humidity and hydrogen sulphide gas present at significant concentrations in biogas. It was determined that the contributing factor to their demise was the build-up of condensation on the methane sensor itself when it was turned off. Therefore, due to the size of the solar panel used in the current study, it was decided to keep the methane sensor powered to reduce the long-term build-up of condensation. During operation, the sensor was placed within an approved intrinsically safe, flameproof gas sensor housing type GSH4-P (Dynament, UK). The sensor was re-calibrated every 3 months and if necessary, adjusted for drift before being deployed.

The CSIRO “Gas” daughter board as deployed on the Lake Wivenhoe and Little Nerang Dam Sensor Networks (Dunbabin & Crossman 2010), was used in this project (Figure 9). Its features include a micro SD card for on-board logging of sensor streams, the provision to interface with two gas (e.g. $CH_4$ and $CO_2$) sensors, a Serial Digital Interface 12 interface for the digital output sensors, RS232 for weather stations, and provision of high resolution ADCs for interfacing with dendrometer bands and soil moisture probes. It also has a Pulse Width Modulation (PWM) output for controlling purging values on the floating gas chambers.

The sensor node, consisting of the sensor daughter board and Fleck™ wireless sensor network board were placed within a waterproof housing (Figure 10) located underneath the solar panel.

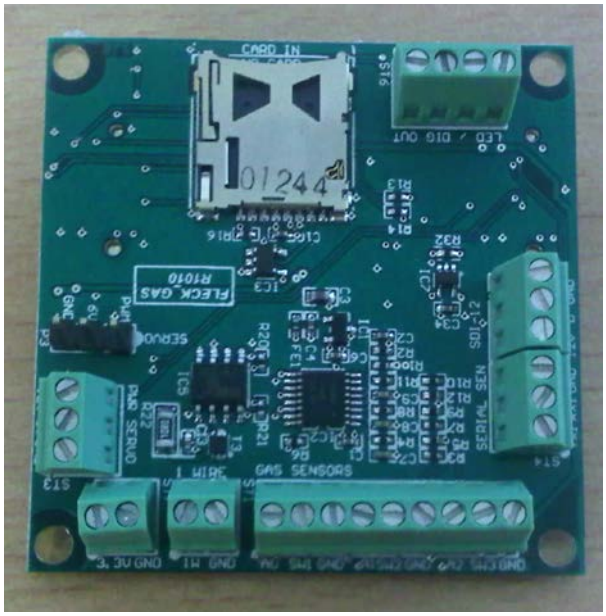


Figure 9 Upgraded sensor interface board for use on floating and land-based sensor networks.

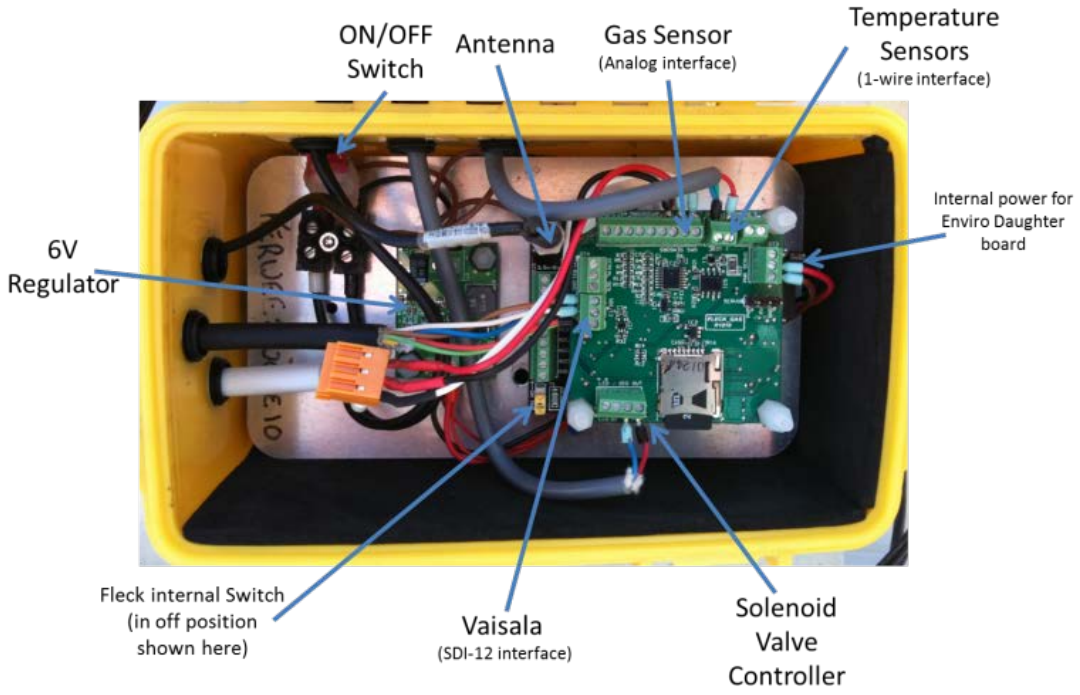


Figure 10 Pond-side wireless sensor network node consisting of a wireless sensor network and Gas daughterboard.

### 5.9.4 Software architecture

The underlying software was based on the Fleck™ Operating System (FOS). The application consists of 3 threads; (1) general watchdog thread, (2) read and send the temperature string data thread, and (3) send the engineering data thread. A simplified flow diagram of the software architecture on-board the Fleck™ 3B is illustrated in Figure 11.

Each node was allocated (hard coded) a unique identification number along with a boot loader program that allowed remote (wireless) uploading of new applications if the need arose.

The primary thread checks for the presence of, and reads the sensors periodically via the SDI-12, RS232 and one-wire interface communication buses. The communication protocol used on each node is the FOS implementation of Link Quality Routing that allows multi-hop data transfer and demonstrated to work in the presence of multiple sink nodes (gateways).

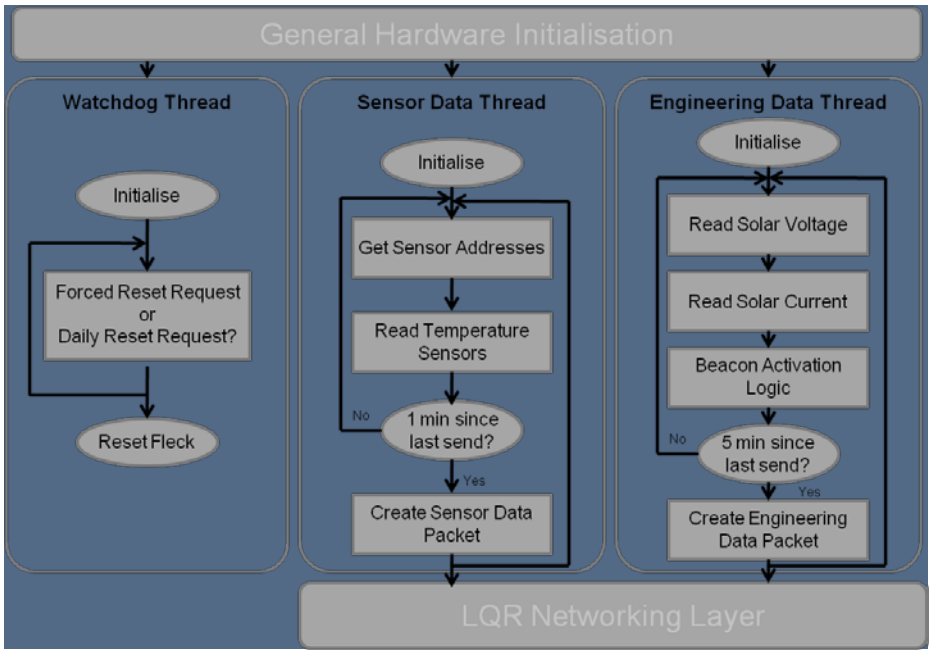


Figure 11 Software architecture of the floating and land-based sensor nodes.

An interactive network must support communications between any, or all of the sensors and robots, as well as human operators. The system (previously developed by the CSIRO sensor network team) uses a light-weight stateless protocol that allows a client running on a host computer(s) or sensor node(s) to seamlessly access services on one or more sensor nodes. Servers are written in C and clients are written in C or Python. Key functionality of the RPC commands on the sensor node include sample rate modification, addition and deletion of a sensor, query any sensor value, list the sensors, and set the node ID number.

A final addition to the software architecture compared was a routine to monitor and purge the floating chambers.

### 5.9.5 Gateway Node

There is a single gateway node at Kerwee located in the feedlot shed/office approximately 400 m from the pond. The gateway provided the interface between the meshed sensor

network and the remote database via 3G-network and the Internet. It also provided the interface for Remote Procedural Calls to be sent to the network nodes. All sensor traffic within the network was funnelled into the gateway, which then locally buffers before forwarding it on to the database. Details for the remote access (MAC address and mobile number) for the Jondaryan gateway node is given in Table 1.

Table 1 Gateway remote access details.

| Gateway location | MAC Address | Mobilenet number |
|---|---|---|
| Jondaryan | 00:0d:b9:1e:a9:00 | 0477300778 |

### 5.9.6 Data Access (Interfaces)

The information flow architecture for Jondaryan allows secure real-time access to data and the in-field hardware by the operators and modellers. Each gateway node has a continuous secure 3G connection to the Queensland Centre for Advanced Technologies (QCAT) where the information is routed into an Oracle database located at the CSIRO Sydney Data Centre. This data can be accessed by authorised operators and modellers via a secure website.

The primary interface is the CSIRO Sensornets website which indicates the current status of the sensor nodes (via colour coding) and allows viewing of the most up-to-date data from the nodes. It also allows the user to view and download historical data from the network in text format. A screen dump of the sensor network interface with the pop-up box for a particular node is shown in Figure 12.

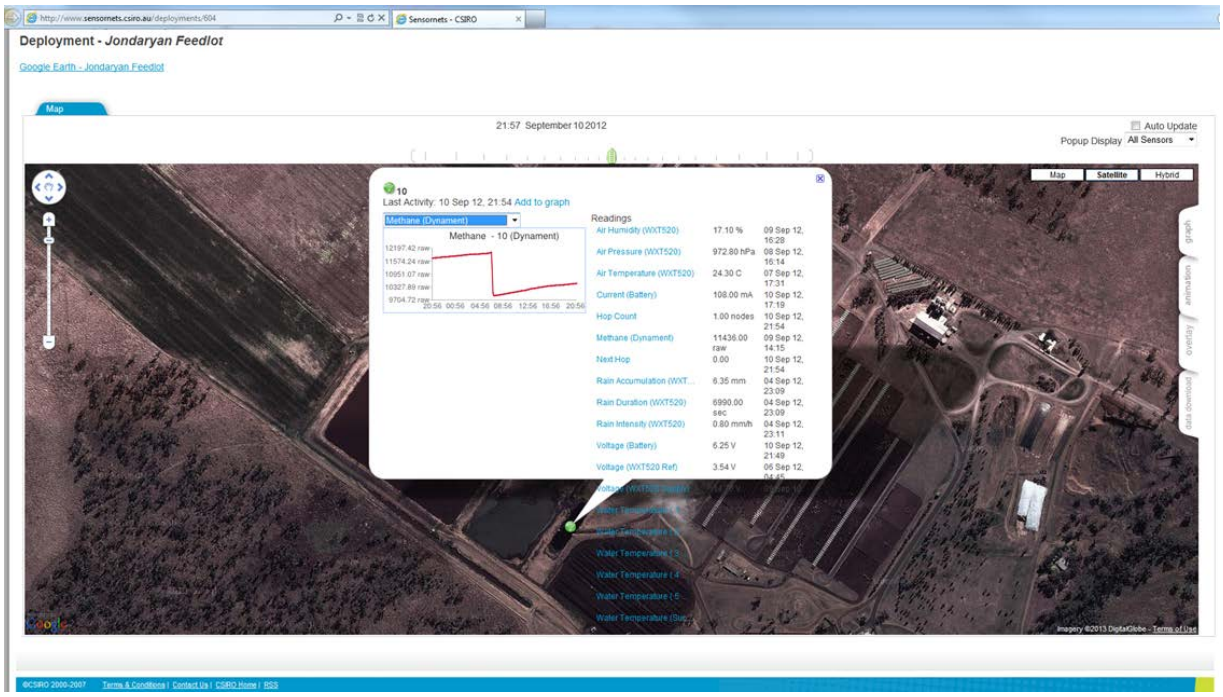


Figure 12 Screen dump of the sensor network website showing a pop-up menu detailing the node's current data and status.

The URL for the Jondaryan deployment on the CSIRO Sensornets website is http://www.sensornets.csiro.au/deployments/604. The sensor network data is considered commercial-in-confidence and therefore a username and password is required to access the database.

## 5.10 Statistical Methods

The objective of the statistical modelling was to characterise the relationship between important climate and environmental variables and the observed methane emission. This is in the format of a preliminary predictive model. With 32 variables recorded over the full time period, model parsimony, interpretability and over-fitting needed to be managed carefully. Hence, appropriate choice of a subgroup of the variables for modelling can significantly reduce time and effort spent during the model development and selection. In this analysis, Random Forests (Breiman, 2001) were used for data-driven variable selection. They offer the ability to rank the importance of variables in a regression problem and hence select the most important variables for further modelling. Regression trees were also used to explore potential variable interactions.

The generalized additive modelling (GAM) technique (Wood, 2006) was the primary tool for analysing the effects of the interactions between climate and environmental variables on methane emission rate. This approach used a flexible regression framework that captured

both linear and non-linear relationships between the climate and environmental variables and methane emission.

### 5.11 Characterising the microbial community of pond sludge using pyrosequencing.

Sludge samples were collected from 16 sites across the pond at three depths (top, middle and bottom; 48 samples in total). Samples were collected on 25th October 2011, 10 days after the last significant influx of substrate from 108 mm of rainfall between 6th - 15th October, 2011.

DNA was extracted from each sample using the PowerSoil kit (MoBio , xx, xxx) and used as the template to prepare 16S ribosomal RNA gene PCR products pyrosequencing by 454 GS FLX sequencer (Roche, Dee Why, NSW). Amplicons were prepared using a modular two-step PCR protocol (Aguirre de Carcer *et al.*, 2011) and primers TX9/1391R with broad specificity for the 16S ribosomal RNA gene of bacteria and archaea. Amplicons were sequenced on the minus strand (i.e. from 1391R towards TX-9). Pyrosequencing data was analysed using UPARSE (Edgar, 2013) and QIIME (Caporaso *et al*., 2010), with sequences trimmed to incorporate variable regions V6, V7 and V8. A total of 10,000 sequences per sample were analysed.

Sequences were clustered into operational taxonomic units (OTU) using a sequence similarity cut-off of 0.97, which is approximately equivalent to a species-level grouping.

# 6 Data and Results

## 6.1 Estimate of available volatile solid in pond sludge and crust

A summary of VS analyses is shown in Table 2. The VS status of the pond did not vary significantly between sampling times that were almost 12 months apart. This would suggest that the pond had a relatively stable VS loading with substrate available for microbial degradation all year round.

The VS of dried crust were also analysed from three separate locations of crust on the pond. These did not differ (VS = 54.7) and indicate that substrate would be available if the crust was subsequently re-submerged. The effect of recent (within 24 h) rainfall and in-flow of fresh substrates on the mean VS of the pond is indicated by a slight increase in the mean and the range of values when compared to previous sampling. VS did not differ significantly with sampling depth or location in the pond. These data suggest that the composition of the substrate was relatively homogenous throughout the pond.

Table 2 Estimation of Volatile solid (VS) as a percentage of dry weight of pond sludge.

| Sample | n | VS (% Dry Wt) | SD | Range |
|---|---|---|---|---|
| Sludge (Oct 2011) | 51 | 54.9 | 4.7 | 37.1 – 60.6 |
| Sludge (Sept 2012) | 15 | 54.9 | 2.9 | 49.7 - 58.0 |
| Sludge (Oct 2012)* | 13 | 55.6 | 3.6 | 48.1 – 64.1 |

- Sludge was sampled after a 108 mm rainfall event.

## 6.2 Methane emission: monthly summary

A total of 650 estimates (individual capture-purge cycles) of methane emission were recorded over the experimental period. The frequency of cycles ranged from less than one cycle per day during the colder months between April and September, peaking in frequency to more than 18 cycles per day during January/February 2013. The cycle rate is reflected in Figure 13 where the rate of methane emission is clearly seasonally influenced; highest in the wetter warmer months of the year (January to March 2013) and lowest in the drier cooler months (June to September 2012). More detail on the influence of climatic variables on methane emission is provided below in Section 11.4 to Section 11.6.

During the period 27$^{th}$ Apr - 30$^{th}$ Sept 2012, there were 65 daily estimates of daily methane emission rate (monthly average is shown in Figure 13) recorded with a mean (± se) of 18.19 ± 0.94 g $CH_4/m^2$ surface area/d. In contrast, there were 96 daily estimates of daily methane emission rate recorded between the 1$^{st}$ Oct, 2012 to the 26$^{th}$ April, 2013 with a mean (± se) of 164.69 ± 10.34 g $CH_4/m^2$ surface area/d. The overall mean (± se) emission rate for the year was 94.59 ± 7.50 g $CH_4/m^2$ surface area/d.

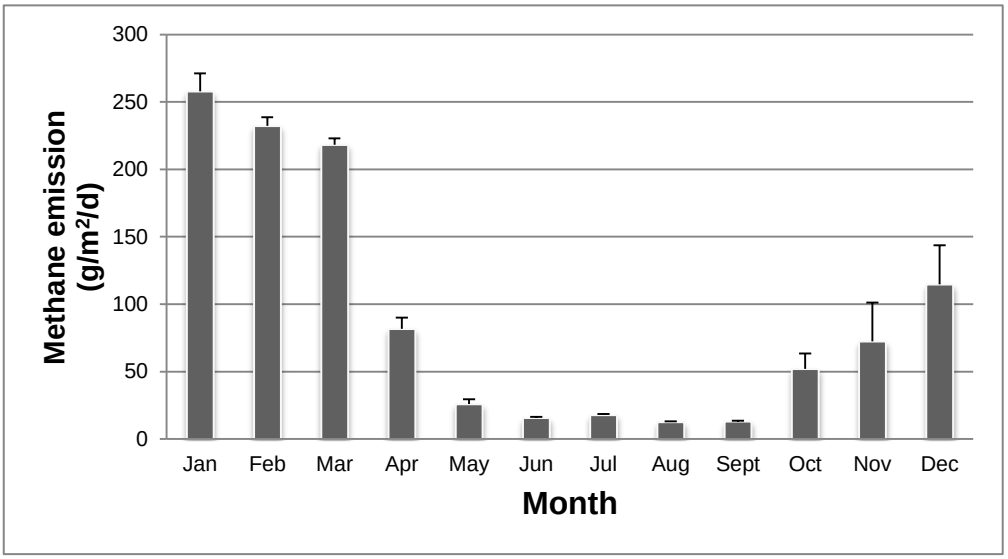


Figure 13 Summary of monthly average (+/- SD) methane emission rate from a feedlot anaerobic pond.

## 6.3 Biogas composition

The air-free concentration of three of five replicates could not be determined due to spurious data and were subsequently discarded. The breakdown of the remaining replicates is shown in Table 3.

Table 3 Composition of biogas from a feedlot pond as a percentage air-free.

| Gas | Rep 1 | Rep 2 | Average |
|---|---|---|---|
| **Helium** | 0 | 0 | 0 |
| **Hydrogen** | 0.001 | 0.001 | 0.001 |
| **Carbon monoxide** | 0 | 0 | 0 |
| **Ethylene** | 0 | 0 | 0 |
| **Hydrogen sulphide** | 0.003 | 0.009 | 0.006 |
| **$CO_2$** | 24.760 | 21.668 | 23.214 |
| **Ethane** | 0 | 0 | 0 |
| **Nitrogen** | 1.284 | 1.828 | 1.556 |
| **Methane** | 73.953 | 76.492 | 74.223 |

## 6.4 Climatic and emission data availability and description

Climatic and environmental variables were considered as potentially important predictors of methane emission. The data availability for those variables over the year is summarised in Figure 14. Gaps in the data during December 2012 are an important feature of the data and were as a result of a faulty methane sensor and gas daughter board. Smaller gaps in the data throughout the year were a result of network problems, and sporadic hardware faults at the gateway and the node.

Daily time series plots over the full time period are presented in Figure 15 to capture the range of variability and to provide a sense of the changes that occurred throughout the experimental period. The data are presented on a natural scale with loess smoothers included in blue to provide visual summary of the temporal changes. These plots indicate a strong seasonal variation in the methane emission and associated climate variables. In particular, the time series of water temperature and air temperature have similar patterns to the methane emission rates, indicating that these variables are likely to be significant in terms of predicting methane emission. However, these almost identical time series also suggest possible strong correlations between these climate and environmental variables.

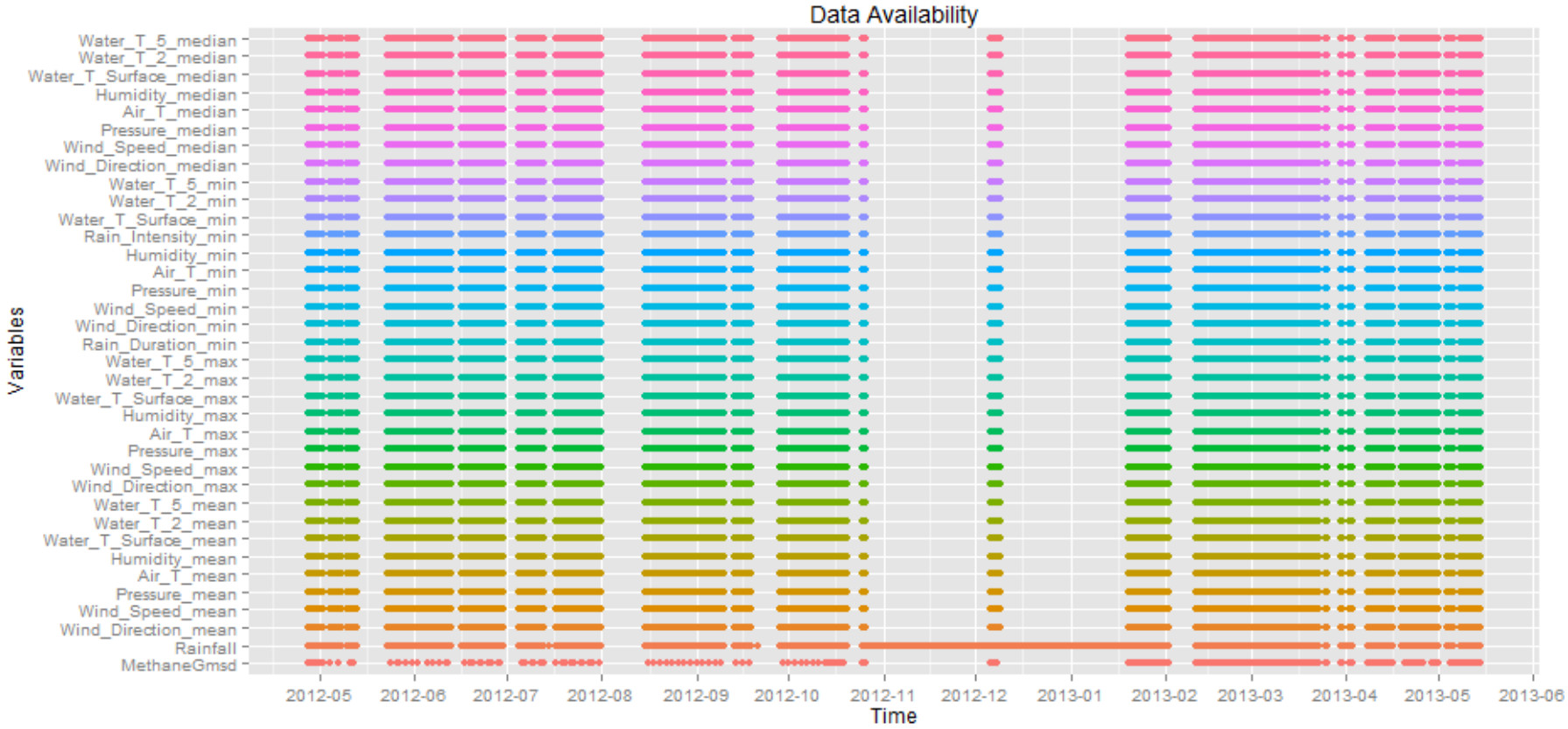


Figure 14 Graphic illustrating the availability of data for all measured variables.

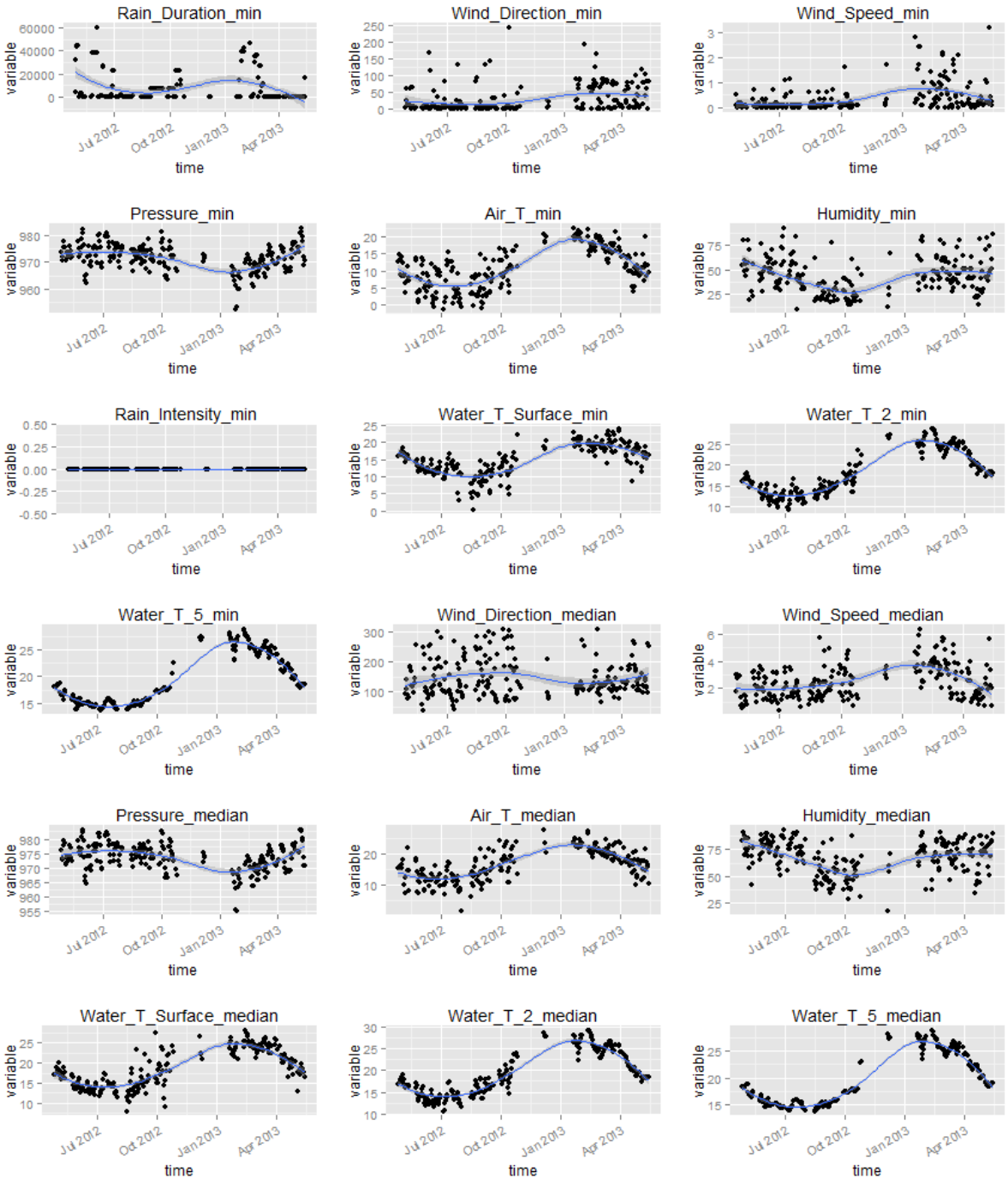
Rain_Duration_min
Wind_Direction_min
Wind_Speed_min
Pressure_min
Air_T_min
Humidity_min
Rain_Intensity_min
Water_T_Surface_min
Water_T_2_min
Water_T_5_min
Wind_Direction_median
Wind_Speed_median
Pressure_median
Air_T_median
Humidity_median
Water_T_Surface_median
Water_T_2_median
Water_T_5_median
variable
time
Jul 2012
Oct 2012
Jan 2013
Apr 2013

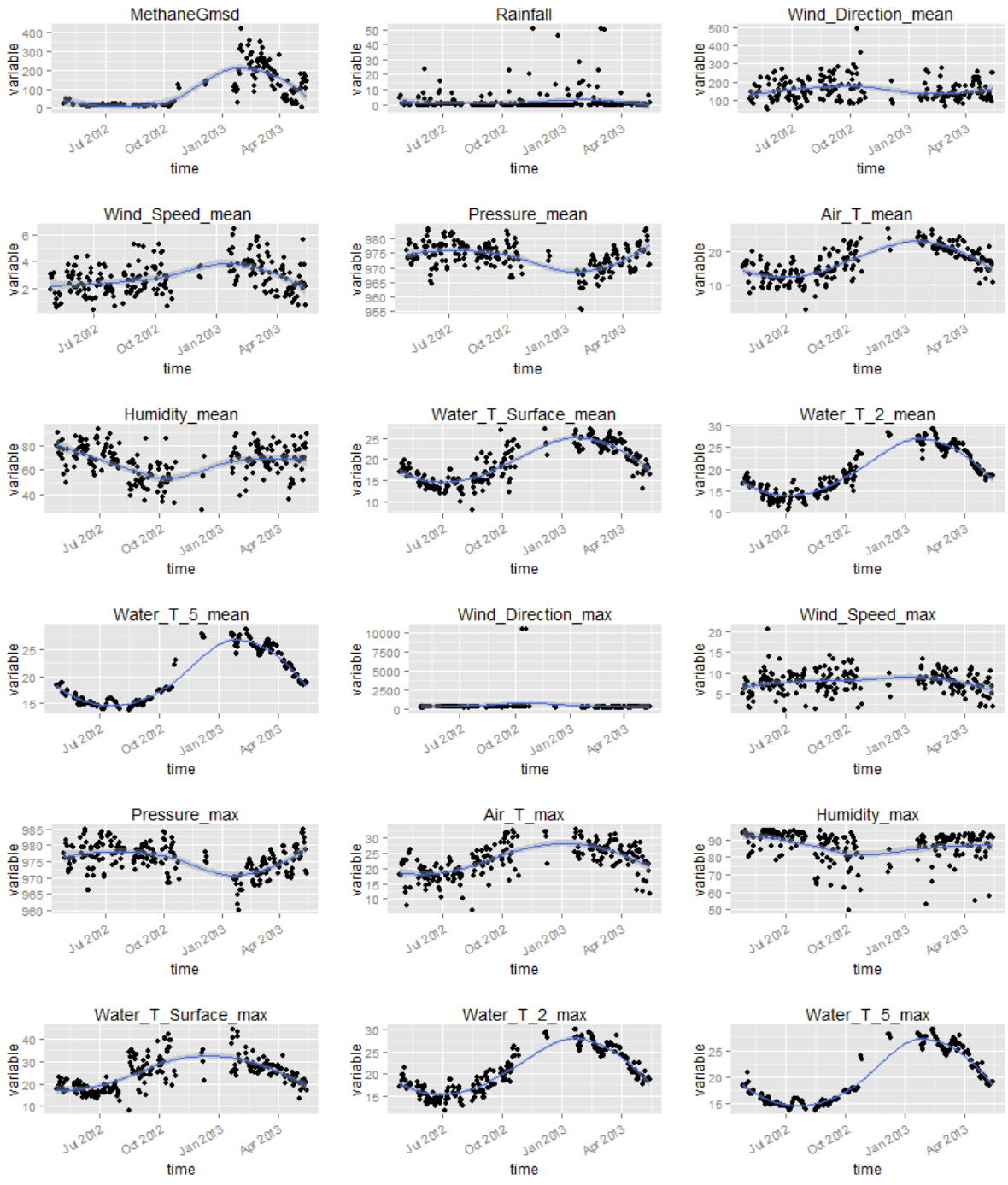


Figure 15 Daily time series plots over the experimental period presented to capture the range of variability in environmental variables. Water_T2 and T5 are the temperatures in °C at ~0.75 m and 2.20 m within the water column.

Water temperatures were recorded at six different depths in the water column, though only the surface, T2 (~ 0.75 m) and T5 (~ 2.20 m) are considered further given the strong

correlations between them (Figure 16). Maximum temperature at the water surface of the pond is consistently higher than the maximum temperature at T2 and T5 depths throughout the year. Conversely, the water surface minimum temperature is consistently lower than the minimum temperature at T2 and T5 depths for the year. This is expected given the fact that the thermal conductivity of water is relatively low. The difference in mean and median temperatures at different depth is minimal, especially in winter months. In summer months, however, the water surface temperature (both mean and median) is lower than T2 and T5 depths. Again, explained by the water thermal conductivity.

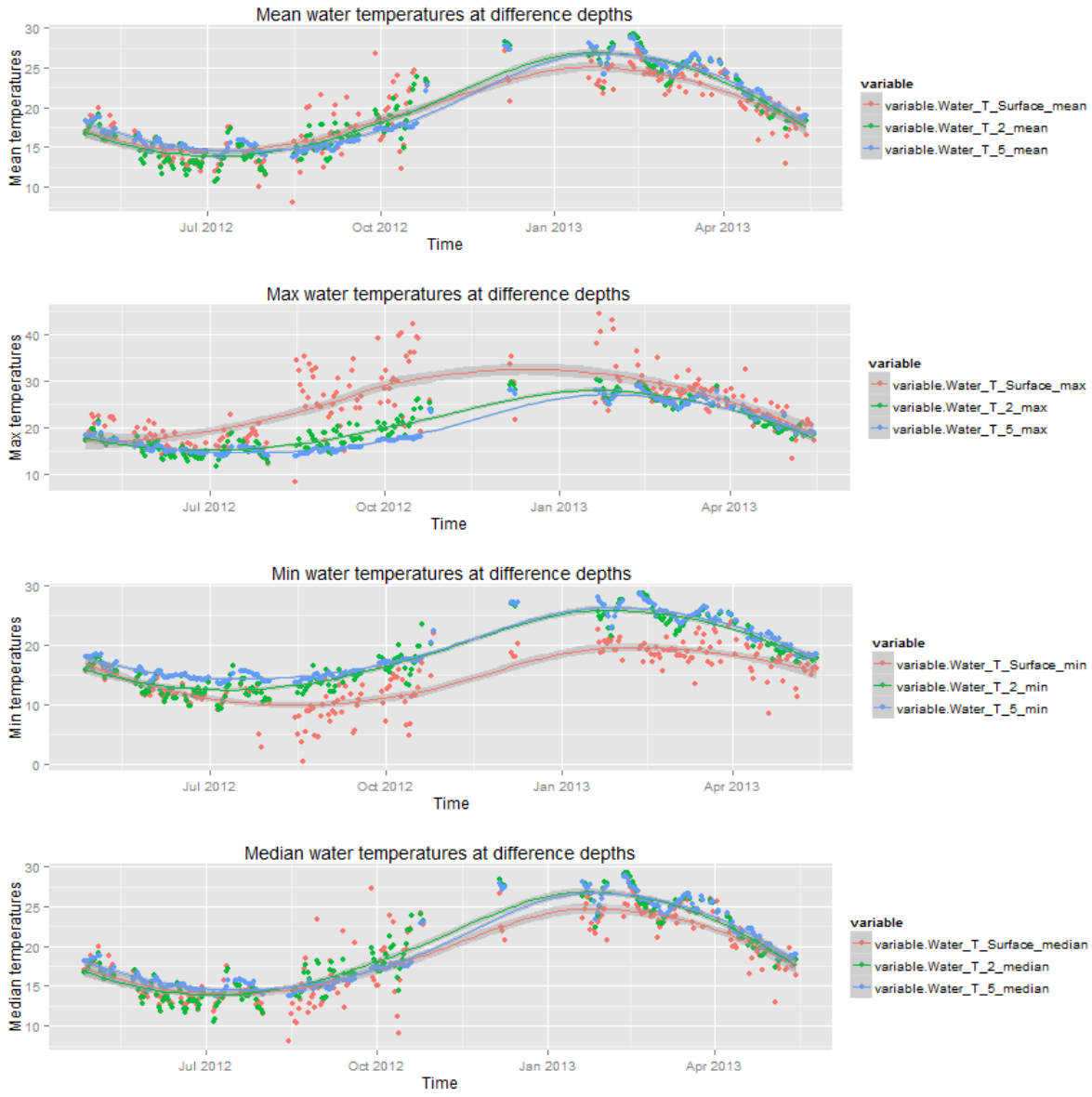


Figure 16 Time series plots for water temperatures ( C) at the pond surface and at depths of 0.75 and 2.20 m Water_T2 and T5 respectively) over the 12-month period 27 April 2012 to 27 April 2013. Loess smoothing was used to provide summaries of the trend to aid in visualisation of the pattern.

Daily rainfall data from the Kerwee feedlot and from the pond weather station for the time period between the 27th April 2012 and 27th April 2013 was incomplete. Data was obtained from the Bureau of Meteorology (BoM) for Jondaryan post office as representative of the area at only ~ 5 km from the feedlot and the data combined to form a complete log of rainfall during the period. The daily rainfall data was converted to 7-day accumulated rainfall (sumrain) prior to analysis for methane emission rate. Although this accumulation results in some loss of information, the 7-day period was appropriate in representing the lag between rainfall event and methane emission response. Other potential periods of aggregation were considered but are not described further here.

## 6.5 Variable Selection using Random Forest

Random Forest analysis was used to identify the most important variables for predicting methane emission rate. Ranking of their importance is shown in Figure 17. Of these, *Water_T_5_median* had the highest rank in terms of prediction.

In order to reflect the impact of antecedent rainfall on methane emission, accumulated rainfall (sumrain, mm) over the past week was considered to have a significantly higher impact on methane emission rate than did daily rainfall.

Briefly, the importance measures show that the mean square error (MSE) node impurity increases when a variable is randomly permuted. When randomly permuted, a variable that does not gain any value in prediction, only small changes in MSE and node impurity will be seen. On the other hand, variables with higher predictive value will change the predictions by a large amount when randomly permuted, so larger changes in MSE and node impurity will be expected and indicate variable importance.

The Random Forest plot suggests that the water temperature and accumulated rainfall are the most important variables. Of the temperature variables, median temperature at greater depth (T5) was ranked highest of all variables and furthermore, was ranked higher than the maximum temperature at all depths.

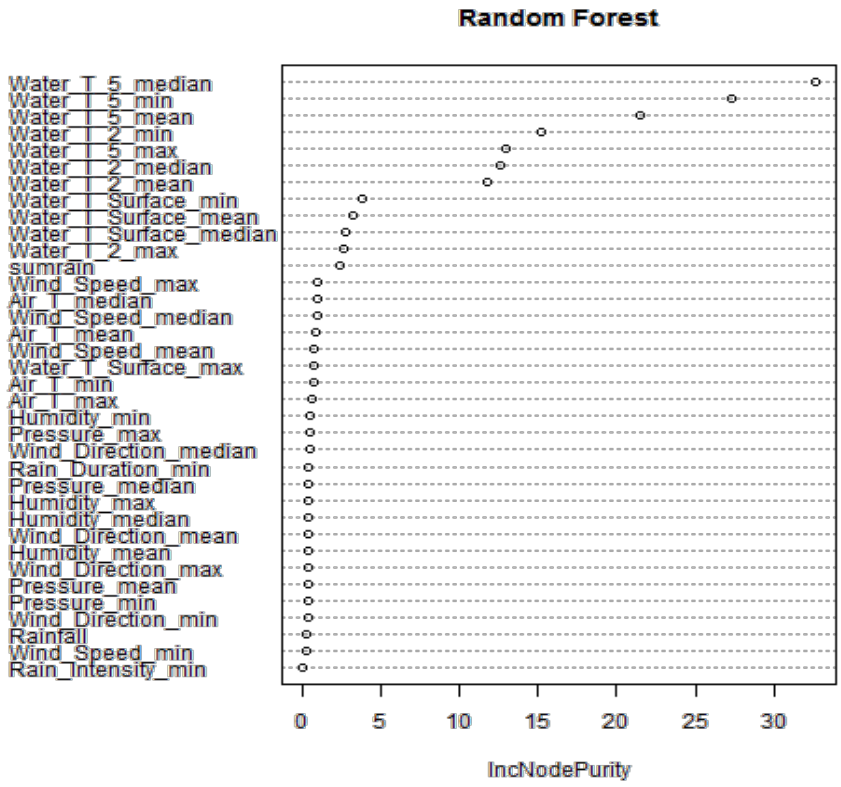


Figure 17 Random forest analysis showing the ranking of variable importance. Values approaching zero indicate variables with little importance.

## 6.6 Generalised Additive Model

### 6.6.1 Correlation and Further Variable Reduction

In order to characterize the relationships between the climate and environmental variables and methane emission rate, the 14 highest ranked important variables given by the random forest (Figure 17) were considered further. A scatterplot matrix for the environmental variables and the methane emission response is presented for reference in Appendix 1. An important feature of these data is that some variables are highly correlated, for instance all temperature related variables show significant associations with each other as would be predicted. This has potential implications for modelling, as parameter estimates of the model can be sensitive when variables are highly correlated with each other, and suggested that further variable reduction was necessary. A selection of variables considered important are summarised in Figure 18.

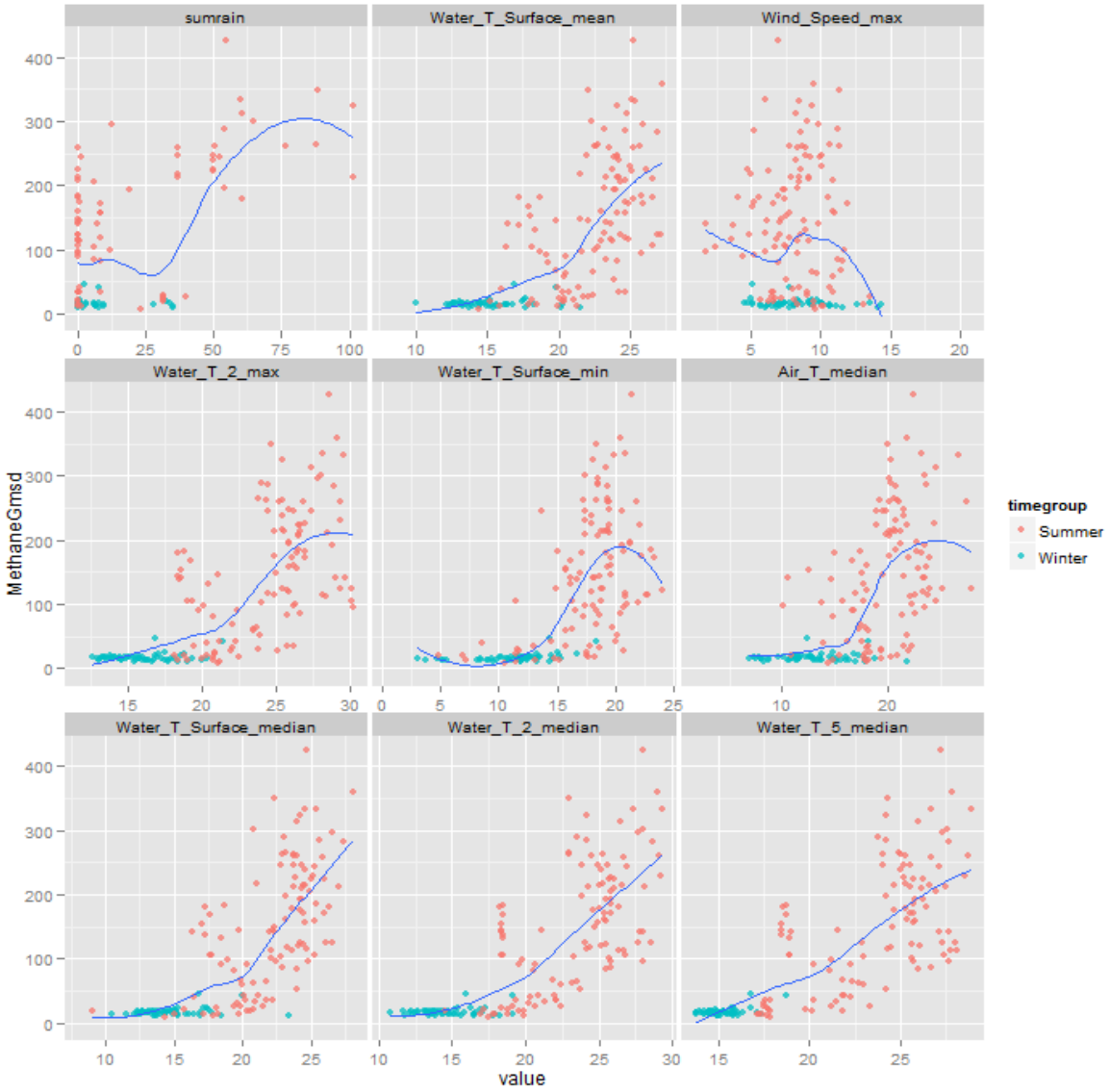


Figure 18 Scatterplots of methane emission rate against important environmental and climatic variables. A scatterplot smoother and symbols for winter (blue versus summer (red) are added for interpretability.

An obvious observation in terms of the methane emission response (Figure 18) is that there is a similar response pattern indicated between the emission rate (*MethaneGmsd*) and all the environmental variables except for *Wind_Speed_max*. More explicitly, the clusters of colour clearly represent a seasonal separation of the data recorded; cooler winter months (blue, April 2012 to September 2012) and warmer summer months (red, October 2012 to March 2013). In winter, both water and air temperature are relatively low and stable thus variability of methane emission rate is little influenced by these variables. In summer there is a strong positive relationship between methane emission rate and the selected

environmental variables. In comparison Wind speed however, does not vary significantly itself.

It is clear that a simple linear fit does not describe these data, particularly for the variables *sumrain*, *Water_Surface_mea*n, *Water_Surface_max*, *Water_Surface_min* and *Air_T_median*, where a nonlinear relationship is indicated.

### 6.6.2 Generalised Additive Model

An initial generalised additive model for this data was fitted, using variable selection based on the random forest modelling after removing some of the highly correlated variables, and considering the methane emission response on the log scale.

The significance level of individual variables is given in Appendix 2 with other measures of fit also reported, such as the adjusted $r^2$ and percentage deviance explained, along with the GCV score, an estimate of the scale parameter of the model, and the number of data fitted.

The model indicates a good fit in every aspect, especially considering 95% of the deviance is explained, despite some variables not being significant. This suggests a strong correlation between variables. It was noted that the terms *Wind_Speed_max*, *Water_T_2_max*, *Water_T_Surface_median* and *Water_T_2_median* have effective degree of freedom (edf) 1, indicating that these variables are linearly related to the response in this particular model.

Although a good model, interpretability is still poor due to the large number of variables, and alternative models deliver a similar predictive ability. It is difficult to explain the contributions of individual variables to the model given complex interactions between highly correlated variables. Figure 19 shows the estimated effects as solid lines/curves, with the 95% confidence limits shown as shaded areas.

It is clear that *Water_T_2_mean* and *Water_T_Surface_mean* have been reduced to a linear fit and have some positive effect but are not significant. The third panel in the second row of Figure 19 illustrates the contribution of *Air_T_median* to methane emission rate response after all the other variables have been accounted. The negative relationship observed here is in contrast to a positive but marginal relationship inferred by the scatterplot matrix in Figure 18.

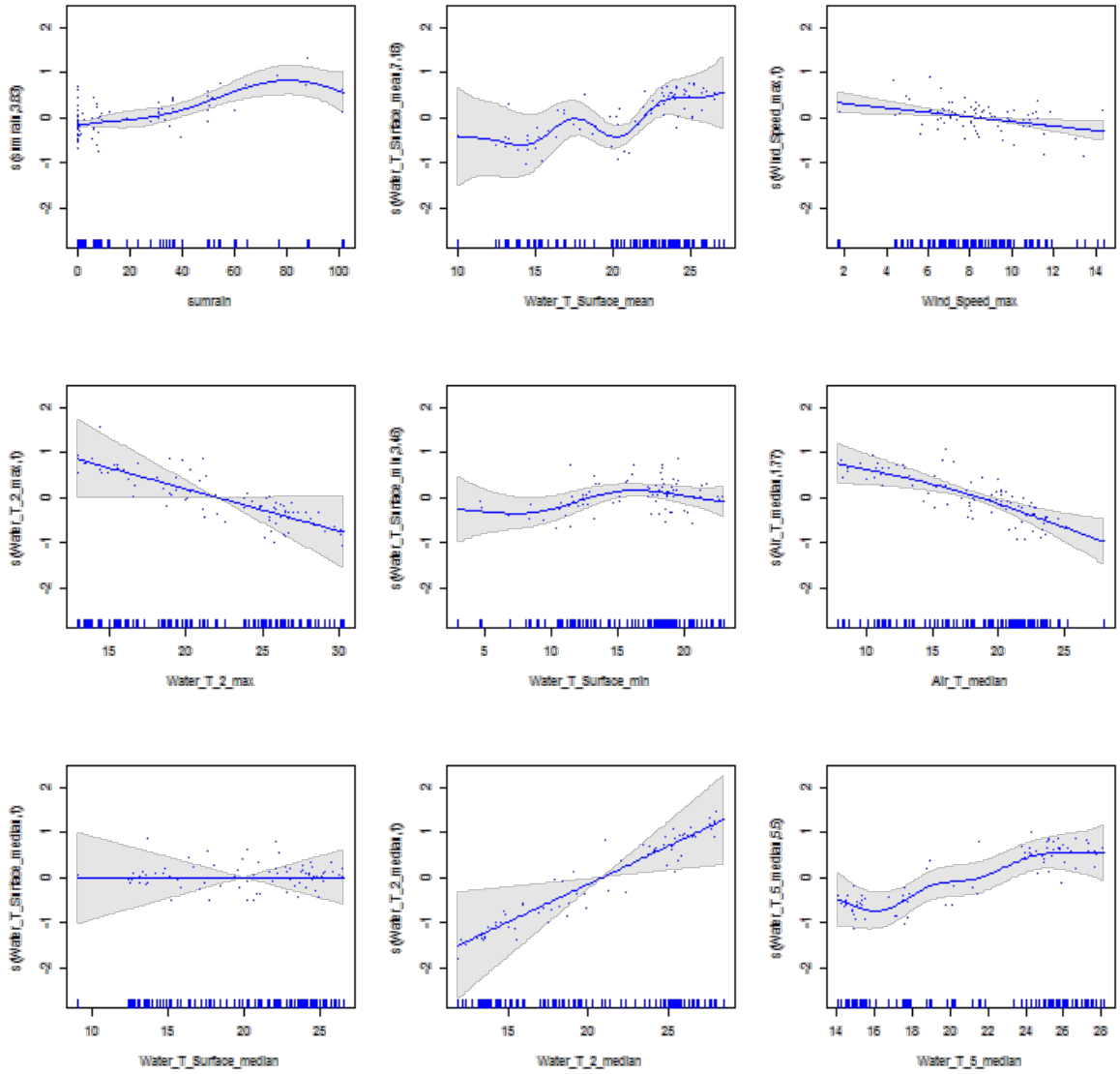


Figure 19 Contribution to a fitted model by environmental and climatic variables. Note that these are the partial contributions, after having adjusted for other terms in the model.

### 6.6.3 Towards a simplified Generalised Additive Model

Regression trees were considered as a way to investigate important variable interactions and reduce some of the model complexity. The fitted regression tree for the observed methane emission rate based on the same set of variables used in the initial generalised additive model is shown in Figure 20.

Qualitatively, the tree plot does a good job of capturing the interaction between the environmental variables. It can be viewed as a decision tree where at each internal node, we ask the associated question (as labelled), and go to the left if the answer is yes, to the right if

the answer is no. The number at the bottom of each end node represents the average of methane emission (g/m$^2$/d) in that cluster.

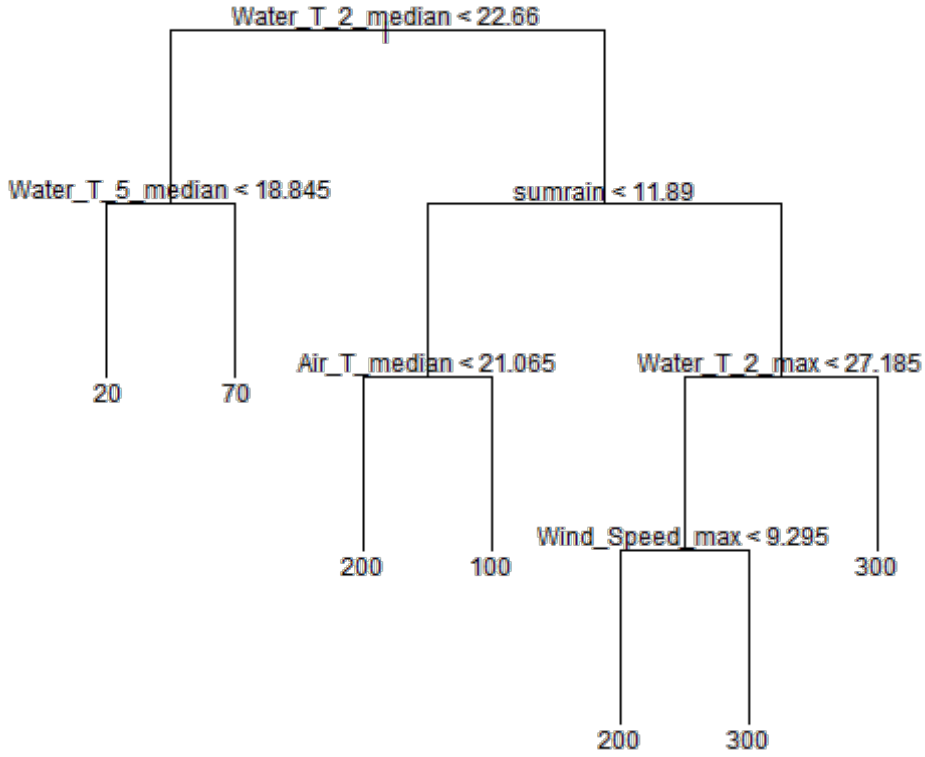


Figure 20 Fitted regression tree for methane emission rate over the annual cycle (winter and summer data combined).

The following observations can be made:

1. If *Water_T_2_median* is high, regardless of temperature at lower depth, methane emission will be relatively high. Lower depth temperature level is only important when the upper level temperature is low. Note the variation in *Water_T_2_median* is relatively consistent with changes in season. This suggests that it would be appropriate to model summer and winter separately.
2. At high *Water_T_2_median*, the accumulated rainfall is positively correlated with methane emission.
3. Wind speed is positively correlated with the methane emission when rainfall amount is large and the water T2 temperature is high but relatively stable.
4. When rainfall amount is small, air temperature becomes important. This indicates that when water temperature is high, *Air_T_median* is negatively related to methane emission. In other words, when water is warm and rainfall amount is small, lower air temperature will lead to larger methane emission.

Considering only the interaction term between *Water_T_2_median* and accumulated rainfall (*sumrain)*, given their importance in the regression tree and the initial generalized additive

models, provides a simple generalised additive model. The model is a good fit (83% deviance explained) and has excellent interpretability, as illustrated in the contour plot (Figure 21). Methane emission clearly increased with warmer temperatures and with greater accumulated rainfall. For accumulated rainfall greater than 35 mm a similar emission rate is delivered for water temperatures that can be greater than 5 ˚C cooler. A more detailed model output providing the significance of each variable in the model is given in Appendix 3.

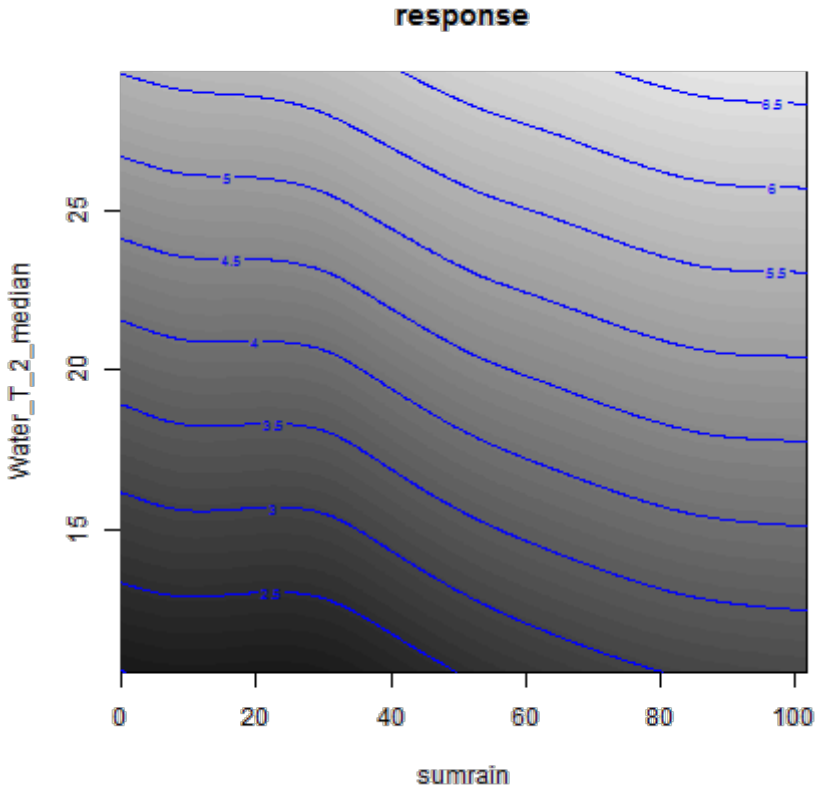


Figure 21 Image plot of predicted log methane emission rate as a bivariate function of median water temperature (C) at 0.75 m and the accumulated 7-day rainfall (mm). Note the log scale of the contour lines. Dark colours represent low methane emission rates.

### 6.6.4 Seasonal specific models

Previous analysis suggests that there is a significant difference in data between seasons. In this section the data has been divided into the two major seasonal influences: winter months (April 2012t o September 2012) and summer months (October 2012 to March 2013). Here the same model was applied to both data and results compared. The output suggests that the summer model is a much better fit than winter (explaining 68.2% deviance in summer compared to 31.6% in winter), indicating that the methane emission rate is more responsive to environmental variables in summer months. This feature is indicated in a comparison of

contour plots for summer and winter with accumulated rainfall (sumrain) on the x-axis and *Water_T_2_median* on the y-axis presented in Figure 22.

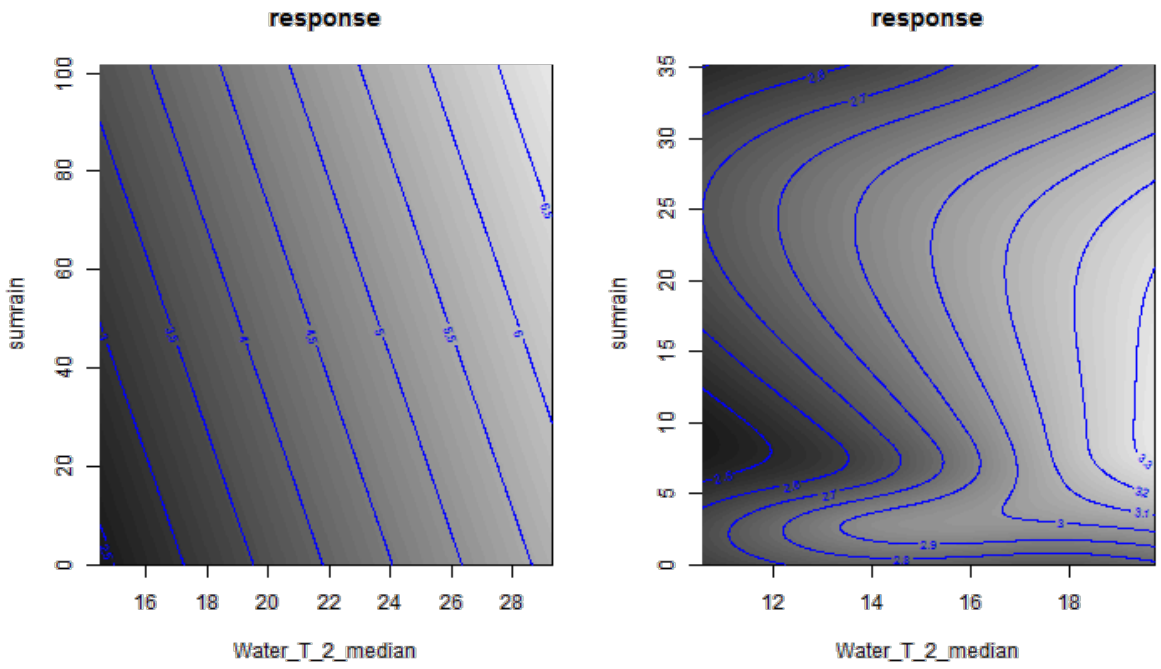


Figure 22 Contour plots showing the difference in methane emission response in Winter (right plot) and Summer (left plot).

It is clear that the relationship between the environmental variables and methane emission in summer was different from that of winter. In summer, as expected, both accumulated rainfall and water median temperature have positive relationships with methane emission. In contrast, the winter response is the opposite. Further, in winter, if the rainfall amount is relatively small, the water temperature has almost no effect on methane emission (the contour lines are nearly flat on the bottom of the right panel).

The difference between the regression trees for summer and winter data is further illustrated in Figures 23 and 24.

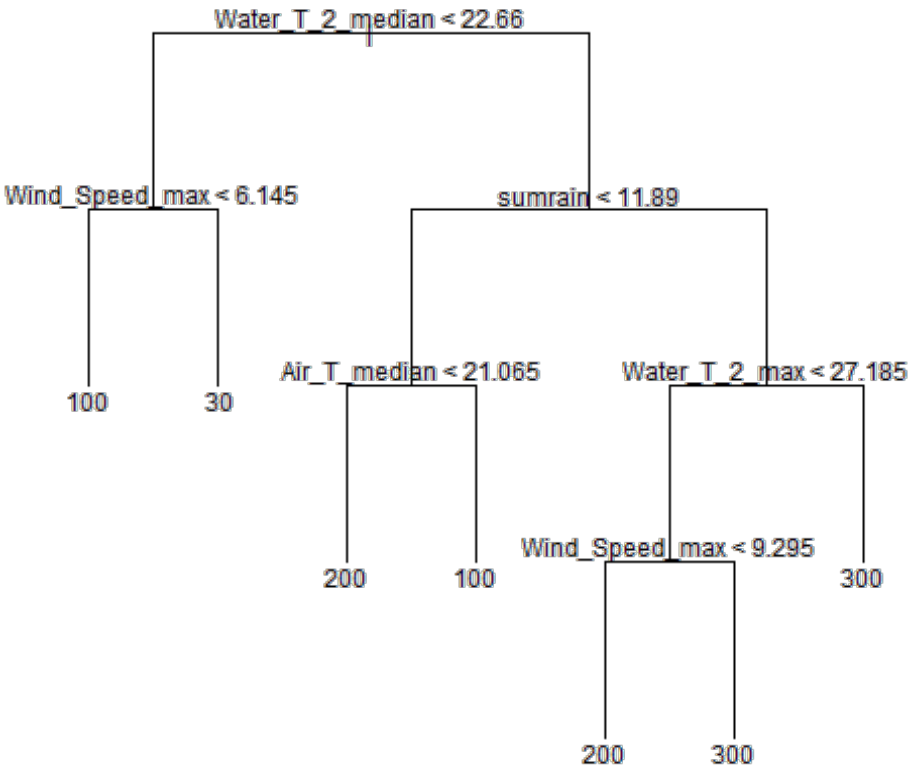


Figure 23 Fitted regression tree for summer (only) methane emission rate.

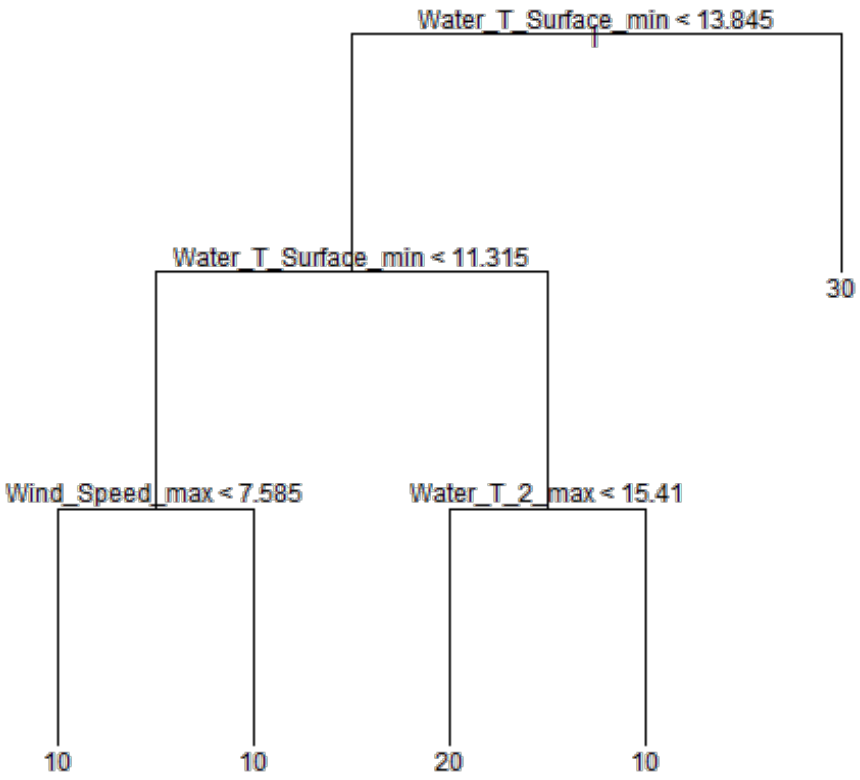


Figure 24 Fitted regression tree for winter (only) methane emission rate.

From the separate summer and winter modelling, the following observations can be made:

1. In summer, mid and lower level water temperature medians and accumulated rainfall (sumrain) is important. This is consistent with the overall modelling result;
2. In winter, the opposite seems to be true - the surface water temperature maxima or minima is important.
3. The fact that the summer tree plot (Figure 23) has similar features to that of the combined season tree plot (Figure 20) would indicate that the relationships observed between the environmental variables and methane emission rate were influenced largely by the effects of summer.

## 6.7 Microbial community in feedlot pond sludge.

Approximately 85% of the sequences were bacterial in origin, while the remaining 15% were archaeal. The bacterial community of the sludge was dominated by sequences from the Chloroflexi (29.5%), Firmicutes (20.1%), Bacteroidetes (11.2%), Proteobacteria (7.6%), Actinobacteria (4.9%) and the Synergistetes (1.9%). Sequences from more than 10 additional phyla each represent less than 1% of the total dataset.

The predominant archaeal OTU contained 10.9% of the total sequences and was representative of the genus *Methanosaeta*, acetoclastic methanogens that can only make methane from acetate. *Methanosaeta* spp. is common in anaerobic digesters (Pope *et al*., 2012) but are rarely found in the gastrointestinal tract of ruminants (Janssen and Kirs, 2008). This would suggest that the source of the methanogens was environmental (soil) rather than from the manure. A diversity of methanogens from the orders Methanomicrobiales and Methanobacteriales were present at lower abundance, suggesting that a proportion of the methane produced is hydrogenotrophic in origin. Additionally, 1.5% of the total sequences were assigned to the Crenarchaeota, a non-methanogenic lineage of the phylum Archaea.

Phylogenetic profiling of the feedlot pond indicates that it contains significant biodiversity. The community is capable of co-ordinating a wide range of biochemical functions that lead to production of substrates for methanogenesis. Many of the OTUs are unrelated to cultured bacterial isolates, suggesting that much of the functional diversity in this system remains undefined. At the time of sample collection, methanogenesis was driven primarily by strict acetoclasts that convert acetate into methane. The presumed source of acetate is microbial breakdown of undigested plant fibre from the pads.

.

# 7 Conclusions

This study has characterised and quantified the seasonal influence on methane emissions from a deep anaerobic sedimentation pond in a feedlot in South-East Queensland.

The methodology and design described herein has demonstrated the feasibility of providing an efficient, remote data gathering, data storage and data management system that can be easily emulated and developed for use in future studies. Despite overcoming the challenges posed by the energy requirements of an on-demand 12 V system, and considering the reliability of the 3G-network in rural Australia, this study has provided a floating sensor capability readily re-locatable to a variety of production systems (e.g. Dairy slurry ponds) and geographical locations. The platform capability has facilitated the collection of an easily accessible, high quality environmental data resource for future scientific use as a major outcome. Furthermore, the platform is amenable for adapting technologies (e.g. metal organic framework technology; Dr Matthew Hill, personal communication) as a natural progression in the research and development of strategies to collect, enrich and harness methane as a renewable energy resource.

Methane was emitted from the surface of the pond all year round although daily emission rates were influenced significantly by seasonal factors combined with in-flow of fresh substrates into the pond during several major rainfall events. The range in rates of emission of methane observed in this study was consistent with the published range (21.0 – 54.8 $g/m^2/d$; Craggs *et al*., 2008; Minato *et al*., 2012) while higher values extend the upper limit. The wider range observed in the current study is undoubtedly a consequence of climatic differences between South-East Queensland and that of the North Island of New Zealand and Hokkaido in Japan, where the previous studies were undertaken.

The climatic data would suggest that seasonal conditions over the period were not markedly different from previous years, although against the 50-year average, the feedlot experienced a marginally warmer winter and a slightly cooler summer. The data confirmed the predicted strong correlation between all temperature variables. Moreover, after accounting for these interactions, modelling discerned clear seasonal proclivities towards summer where the mid and lower water column temperature medians, and accumulated rainfall (provision of fresh substrates), were shown to be major factors driving the methane emission response. In contrast, the opposite was true in winter where the upper level water temperature extremes, maximum and minimum temperatures were important.

Together, these data are consistent with the predicted effects of temperature and substrate concentration on the growth dynamics of microbial populations and the release of by-products of fermentation such as biogas. The composition of the biogas from the pond was similar to that described in the literature (Zhongtang et al., 2010) for manure feedstock. It is important to consider that the biological data provide a snapshot of the microbial community at a defined point in time. Clearly, the dominant methanogens present in the sludge were not remnant of the rumen but are the predominant methanogens found in anaerobic digesters. A targeted metagenomic study over an extended time period could uncover novel

opportunities to enhance methane production by optimising delivery of substrates and controlling the activities of specific microbial cohorts.

In brief, a synthesis of the methane and climatic data reported here was modelled against theoretical and estimated methane yield data to determine the VS required to providing the yield of methane observed. These data suggested that ~17% of the excreted VS at the feedlot would need to have entered the pond to equate to the observed yield of methane reported. This was higher than the 2% estimated as a typical amount believed to be entrained in feedlot pad runoff. Several caveats were attached to the apparent over-estimation of the data including 1) prior historical VS in the pond, 2) a higher methane potential of the leachate in the runoff, 3) under prediction of the maximum methane yield and methane conversion factor (MCF) and 4) an overestimation of the emitting surface area.

Both datasets were subsequently assessed in economic evaluations of different scenarios: a covered anaerobic pond (CAP) and a combined heat and power (CHP) system. Neither system was shown to be an economically feasible strategy at the Kerwee feedlot. This was largely a function of the huge variability in methane emission observed throughout the year, predicated on season and random rainfall events to provide ideal conditions and fresh feedstock to the pond to stimulate emission. However, the report also considered a constant feed scenario where the manure feedstock was applied directly to the pond. Under these circumstances, but within defined limits of manure handling costs ($5-14/tonne), a CAP and boiler system or CHP would be an economically feasible option. Further detail of this assessment is provided in the accompanying report provided under contract to FSA.

Development of strategies, such as metal organic framework technologies to enrich, scrub and store methane/ biogas collected from a CAP system, is an obvious and logical extension to this work. Furthermore, knowledge gleaned from studies of the microbial populations in anaerobic ponds will improve the efficiency of fermentation by selecting and seeding appropriate microbial communities to further increase the yield of methane in natural anaerobic digester systems.

# 8 Bibliography


Aguirre de Carcer, D., Denman, S.E., McSweeney, C. and Morrison, M. (2011) Strategy for modular tagged high-throughput amplicon sequencing. *Applied and Environmental Microbiology* **77**, 6310-6312

Breiman, L. (2001). "Random Forests". *Machine Learning* **45**, 5–32. doi:10.1023/A:1010933404324

Caporaso, J.G., Kuczynski, J., Stombaugh, J., Bittinger, K., Bushman, F.D., Costello, E.K. et al. (2010) QIIME allows analysis of high-throughput community sequencing data. *Nature Methods* **7,** 335-336.

Craggs R., Park J., Heubeck S. (2008). Methane emissions from anaerobic ponds on a piggery and a dairy farm in New Zealand. *Australian Journal of Experimental Agriculture* **48**, 142-146.

Dunbabin M & Crossman C. (2010) Lake Wivenhoe integrated mobile sensor network: Project summary & general operation manual. *Seqwater internal report*, CSIRO ICT Centre.

Edgar, R.C. (2013). UPARSE: Highly accurate OUT sequences from microbial amplicon reads. Nature Methods epub ahead of print dx.doi.org/10.1038/nmeth.2604

Food and Agriculture Organisation of the United Nations (FAO) (2009).

Fujino J., Morita A., Matusoka Y., Sawayama S. (2005). Vision for utilisation of livestock residue as bioenergy resource in Japan. *Biomass and Bioenergy* **29**, 367-374.

Ghafoori E., Flynn P. C., Checkel M.D. (2006). Global warming impact of electricity generation from beef cattle manure: A life cycle assessment study. *International Journal of Green Energy* **3**, 257-270.

Janssen, P.H. and Kirs, M. (2008) Structure of the archaeal community of the rumen. *Applied and Environmental Microbiology* **74**, 3619-3625.

Loh Z, Chen D, Bai M, Naylor T, Griffith D, Hill J, Denmead T, McGinn S, Edis R (2008). Measurement of greenhouse gas emissions from Australian feedlot beef production using open-path spectroscopy and atmospheric dispersion modelling. *Australian Journal of Experimental Agriculture* **48**, 244-247.

Maranon E, Salter AM, Castrillon L, Heaven S, Fernandez-Nava Y (2011). Reducing the environmental impact of methane emissions from dairy farms by anaerobic digestion of cattle waste. *Waste Management* **31**, 1745-1751.

Minato K, Kouda Y, Yamakawa M, Hara S, Tamura T, Osada T (2012). Determination of GHG and ammonia emissions from stored cattle slurry by using a floating dynamic chamber. *Animal Science Journal* pp. 1-13 (doi: 10.1111/j.1740-0929.2012.01053.x).

Moller H. B., Sommer S. G., Ahring B. K. (2004). Methane productivity of manure, straw and solid fractions of manure. *Biomass and Bioenergy* **26**, 485-495.

Neumeier C.J., Mitloehner FM (2013). Cattle biotechnologies reduce environmental impact and help feed a growing planet. *Animal Frontiers* **3**, 36-41.

Pope, P.B., Vivekanand, V., Eijsink, V.G.H. and Horn, S.J. (2012) Microbial community structure in a biogas digester utilizing the marine energy crop *Saccharina latissima*. 3 Biotech dx.doi.org/10.1007/s13205-012-0097-x

Wood S. (2006), *Generalized additive models: an introduction with R*, CRC Press, London.

Yu, Z., Morrison, M., Schanbacher, F.L. (2010) Production and utilization of methane biogas as renewable fuel. Pages 403-429 in *Biomass to biofuels: strategies for global industries*. Edited by Vertes, A., Qureshi, N., Blaschek, H. and Yukawa, H. John Wiley and Sons, UK

Zhongtang Y., Morrison M., Schanbacher F. L. (2010). Production and utilization of methane biogas as renewable fuel. In 'Biomass to Fuels: Strategies for global industries eds. AA Vertes, N Qureshi, HP Blaschek, Yukawa H, Chapter 20, pp 403-433 (John Wiley & Sons, Pty).

# 9 Appendices

**APPENDIX 1** SCATTERPLOT MATRIX OF METHANE, AND ALL ENVIRONMENTAL AND CLIMATIC VARIABLES. POTENTIAL LINEAR RELATIONSHIPS ARE INDICATED BY STRAIGHT LINES AND WERE INVESTIGATED MORE INTENSIVELY.

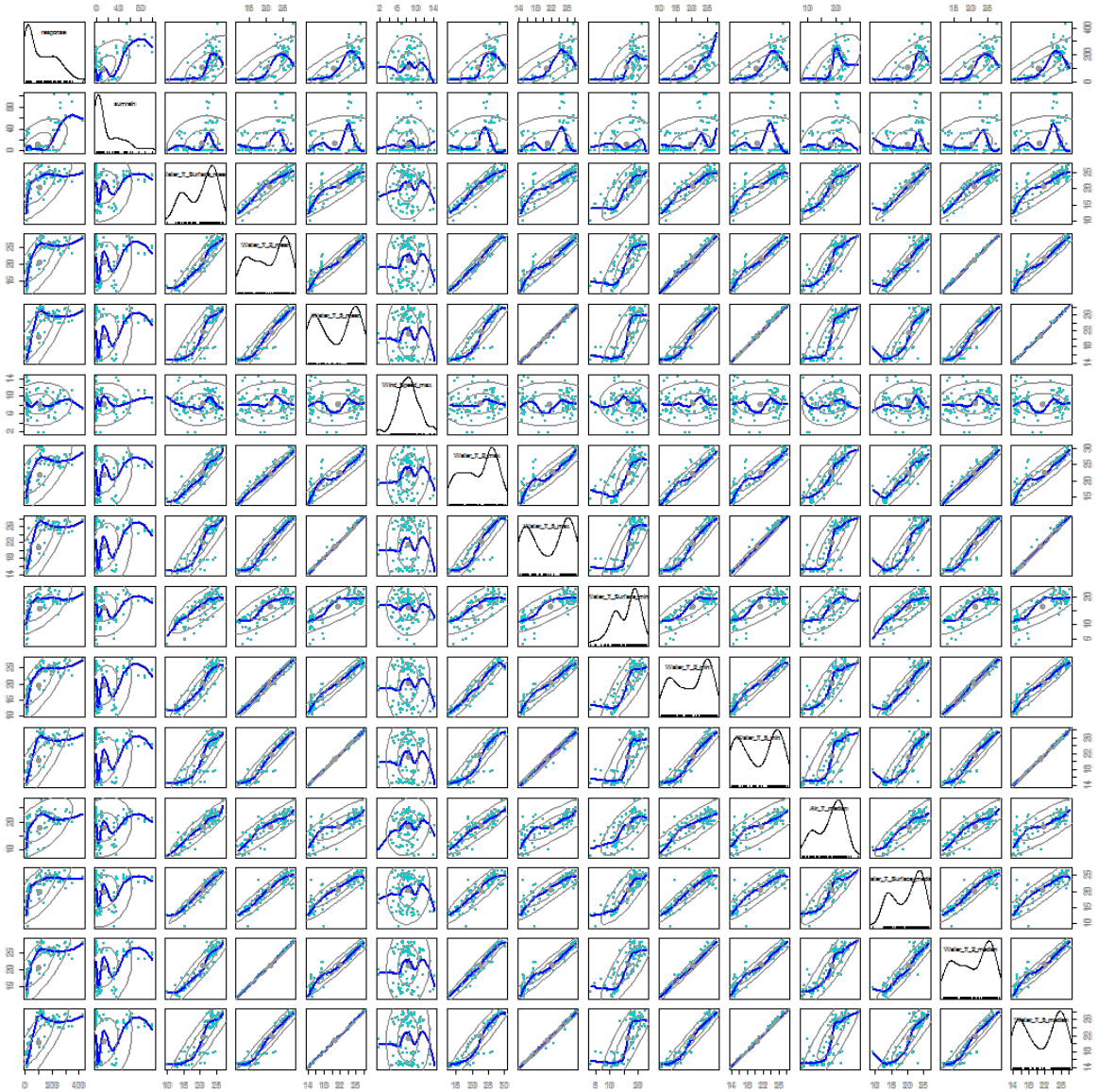

**APPENDIX 2** MODEL OUTPUT FROM INITIAL GENERALISED MODEL SHOWING LEVELS OF SIGNIFICANCE OF THE RELATIONSHIP BETWEEN VARIABLES AND METHANE EMISSION RATE.

```
##
## Family: gaussian
## Link function: identity
##
## Formula:
## log(MethaneGmsd) ~ s(sumrain) + s(Water_T_Surface_mean) + s(Wind_Speed_max) +
##     s(Water_T_2_max) + s(Water_T_Surface_min) + s(Air_T_median) +
##     s(Water_T_Surface_median) + s(Water_T_2_median) + s(Water_T_5_median)
##
## Parametric coefficients:
##             Estimate Std. Error t value Pr(>|t|)
## (Intercept)   4.0926     0.0304     135   <2e-16 ***
## ---
## Signif. codes:  0 '***' 0.001 '**' 0.01 '*' 0.05 '.' 0.1 ' ' 1
##
## Approximate significance of smooth terms:
##                           edf Ref.df    F p-value
## s(sumrain)               3.83   4.65 8.87 1.7e-06 ***
## s(Water_T_Surface_mean)  7.18   8.16 2.93 0.00599 **
## s(Wind_Speed_max)        1.00   1.00 8.03 0.00580 **
## s(Water_T_2_max)         1.00   1.00 3.79 0.05505 .
## s(Water_T_Surface_min)   3.46   4.29 2.15 0.07751 .
## s(Air_T_median)          1.77   2.21 8.64 0.00028 ***
## s(Water_T_Surface_median) 1.00   1.00 0.00 0.97704
## s(Water_T_2_median)      1.00   1.00 6.56 0.01227 *
## s(Water_T_5_median)      5.50   6.66 2.52 0.02353 *
## ---
## Signif. codes:  0 '***' 0.001 '**' 0.01 '*' 0.05 '.' 0.1 ' ' 1
##
## R-sq.(adj) =  0.936   Deviance explained = 95.1%
## GCV score = 0.13159  Scale est. = 0.098698  n = 107
```

**APPENDIX 3** MODEL OUTPUT FROM A SIMPLIFIED GENERALISED ADDITIVE MODEL SHOWING LEVELS OF SIGNIFICANCE OF THE RELATIONSHIP BETWEEN VARIABLES AND METHANE EMISSION RATE.

```
##
## Family: gaussian
## Link function: identity
##
## Formula:
## log(MethaneGmsd) ~ s(Water_T_2_median, sumrain, k = 16)
##
## Parametric coefficients:
##             Estimate Std. Error t value Pr(>|t|)
## (Intercept)     4.09       0.05    81.9   <2e-16 ***
## ---
## Signif. codes:  0 '***' 0.001 '**' 0.01 '*' 0.05 '.' 0.1 ' ' 1
##
## Approximate significance of smooth terms:
##                               edf Ref.df    F p-value
## s(Water_T_2_median,sumrain) 5.37   6.97 72.4  <2e-16 ***
## ---
## Signif. codes:  0 '***' 0.001 '**' 0.01 '*' 0.05 '.' 0.1 ' ' 1
##
## R-sq.(adj) =  0.826   Deviance explained = 83.5%
## GCV score = 0.28401  Scale est. = 0.26709   n = 107
```